

AD A108935

12

LEVEL II

# The Development of High-Intensity Negative Ion Sources and Beams in the USSR

Nikita Wells

12 81

DTIC FILE COPY

296600

DTIC  
ELECTE  
DEC 29 1981  
S D D

DISTRIBUTION STATEMENT A

Approved for public release;  
Distribution Unlimited

Rand

81 12 29 017

The research described in this report was sponsored by the Defense Advanced Research Projects Agency under ARPA Order No.: 3520, Contract No. MDA903-78-C-0189, Director's Office.

The Rand Publications Series: The Report is the principal publication documenting and transmitting Rand's major research findings and final research results. The Rand Note reports other outputs of sponsored research for general distribution. Publications of The Rand Corporation do not necessarily reflect the opinions or policies of the sponsors of Rand research.

UNCLASSIFIED

SECURITY CLASSIFICATION OF THIS PAGE (When Data Entered)

REPORT DOCUMENTATION PAGE		READ INSTRUCTIONS BEFORE COMPLETING FORM
1. REPORT NUMBER R-2816-ARPA	2. GOVT ACCESSION NO. AD-A108435	3. RECIPIENT'S CATALOG NUMBER
4. TITLE (and Subtitle) The Development of High-Intensity Negative Ion Sources and Beams in the USSR		5. TYPE OF REPORT & PERIOD COVERED Technical
7. AUTHOR(s) Nikita Wells		6. PERFORMING ORG. REPORT NUMBER
9. PERFORMING ORGANIZATION NAME AND ADDRESS The Defense Advanced Research Projects Agency Department of Defense Arlington, VA 22209		8. CONTRACT OR GRANT NUMBER(s) MDA903-78-C-0189 ARPA D. W. 35-0
11. CONTROLLING OFFICE NAME AND ADDRESS		10. PROGRAM ELEMENT, PROJECT, TASK AREA & WORK UNIT NUMBERS
14. MONITORING AGENCY NAME & ADDRESS (if different from Controlling Office)		12. REPORT DATE September 1981
		13. NUMBER OF PAGES 65
		15. SECURITY CLASS. (of this report) Unclassified
		16a. DECLASSIFICATION/DOWNGRADING SCHEDULE
16. DISTRIBUTION STATEMENT (of this Report) Approved for Public Release; Distribution Unlimited		
17. DISTRIBUTION STATEMENT (of the abstract entered in Block 20, if different from Report)		
18. SUPPLEMENTARY NOTES		
19. KEY WORDS (Continue on reverse side if necessary and identify by block number) Anions High energy particles Plasma interactions Ion beams Charged-particle beams		
20. ABSTRACT (Continue on reverse side if necessary and identify by block number)  see reverse side		

DD FORM 1 JAN 73 1473 EDITION OF 1 NOV 65 IS OBSOLETE

UNCLASSIFIED  
SECURITY CLASSIFICATION OF THIS PAGE (When Data Entered)

UNCLASSIFIED

SECURITY CLASSIFICATION OF THIS PAGE(When Data Entered)

*by this report*  
Reviews Soviet R&D of (1) high-intensity negative ion sources and (2) transport and focusing of negative ion beams, using Soviet open literature of the past ten years, and correlates this data with data on Soviet institutes responsible for negative ion beam development. The Soviets are developing intense negative ion beams as the basis for creating neutral beams for injection into mirror traps and tokamaks, for inertial confinement fusion, and possibly for exoatmospheric beam weapon applications. The report focuses specifically on surface-plasma-type ion sources, which were first developed in the USSR and which show great promise for creating beams of high intensity, high brightness, and low emittance. Mechanisms for optimum negative ion beam transport are also discussed.

UNCLASSIFIED

SECURITY CLASSIFICATION OF THIS PAGE(When Data Entered)

R-2816-ARPA

# The Development of High-Intensity Negative Ion Sources and Beams in the USSR

Nikita Wells

November 1981

Prepared for the  
Defense Advanced Research Projects Agency



Accession For	
NTIS GRA&I	<input checked="checked" type="checkbox"/>
DTIC TAB	<input type="checkbox"/>
Unannounced	<input type="checkbox"/>
Justification	
By _____	
Distribution/	
Availability Codes	
Dist	Avail and/or Special
A	

DTIC  
ELECTE  
DEC 29 1981  
S D D

PREFACE

This report was prepared in the course of a continuing study, sponsored by the Defense Advanced Research Projects Agency, of Soviet research and development of high-current, high-energy, charged particle beams and their scientific and technological applications. The report examines Soviet research on (1) high-intensity negative ion sources and (2) space-charge neutralization, beam transport, and focusing of high-intensity negative ion beams, as reported in Soviet open-source technical publications. A forthcoming report will discuss Soviet research on the formation of neutral beams by electron stripping of negative ion beams, the development of beam neutralizers, and charge-exchange targets for the conversion of positive to negative ion beams.

The report may be of interest to those dealing with pulsed-power and energy-related research.

### SUMMARY

In 1971, Soviet researchers at the Nuclear Physics Institute in Novosibirsk obtained intense negative ion yields by introducing cesium vapor into a specially designed arc discharge source, which they called a surface-plasma ion source. Thanks to this development and the intense research effort that followed it, the Soviets can now produce high-intensity, high-brightness, low-emittance negative ion beams that are probably on a par with current U.S. achievements for both pulsed and continuous beam operation.

Along with developing surface-plasma ion sources, the Soviets also investigated the transport of negative ion beams through gases at various pressures. This research, carried out largely at the Physics Institute in Kiev, concentrated on ion-beam space-charge neutralization and various beam-focusing mechanisms.

Research on the formation and transport of high-current negative ion beams relates directly to the creation of intense neutral beams for injection into magnetic traps and tokamaks, for inertial confinement fusion, and possibly for exoatmospheric beam weapon applications. The analysis of Soviet developments in ion beam research may thus provide insight into the Soviet capability to develop such weapons. This report presents such an analysis, using data obtained from a survey of Soviet open-source technical publications over the past ten years.

In studying the parameters for optimum operation of the ion sources and the effect of arc discharge conditions on the intensity and quality of the negative ion beams, Soviet researchers have demonstrated that (1) the discharge behavior determines the ion-optical characteristics of the beam and (2) oscillations created by the source discharge can be minimized by adjusting source parameters. Various modifications of the surface-plasma ion source (including semiplanotron and axial hollow-beam versions) have been tried with the aim of improving the control of the source discharge and increasing the power and gas efficiencies. A gas-blocking mechanism created by the presence of

FIGURE PAGE BLANK-NOT FILLED

the plasma in front of the source's emission aperture was found to increase gas efficiency.

The surface-plasma source has produced pulsed  $H^-$  ion beams of up to 1.0 A,  $H^-$  DC beams of 100 mA, and pulsed  $H^-$  beams of over 150 mA with a brightness of up to  $10^8$  A/cm<sup>2</sup>-rad<sup>2</sup>. Stable operation of the hollow-beam surface-plasma source was demonstrated with a projected pulsed  $H^-$  ion beam output of 3 A.

Soviet researchers also investigated negative ion beams produced from Penning ion gauge (PIG) ion sources and determined that the noise of the current oscillations in the negative ion beams was several orders of magnitude lower than the noise in positive ion beams. Work in the USSR on double charge exchange and, especially, on the design and test of charge exchange targets will be reported in a future Rand publication.

In investigating negative ion beam transport through gases at various pressures, Soviet researchers concentrated on the basic mechanisms involved in space charge neutralization of the beam; optimization of beam self-focusing; the study of beam oscillations; and the effects of plasma ion and electron oscillations on beam quality. Probe measurements of the beam potentials and measurements of the positive ion and electron currents created in the beam by the ionization of background gas were made at various locations along the beam and at various gas pressures. At low pressures, these measurements demonstrated the existence of a large positive ion flow along the beam. The flow explains the radial loss of the neutralizing positive ions from the beam. At high pressures, the radial positive ion current was found to be independent of location along the beam and represented by the rate of ion production caused by beam ionization of background gas.

The Soviets conclude that negative ion beams are more easily transported over large distances than are positive beams. They also point out--on the basis of their investigations--other advantages of using negative ions, such as the high efficiency of converting negative ions into neutrals at high energies and the considerably lower current oscillations in negative beams than in positive ion beams. The considerable effort that the Soviets have invested in negative ion beam research, charge exchange targets, and neutralizers implies the continuation of interest of the Soviets in neutral beam production.



ACKNOWLEDGMENTS

I want to thank Theo Sluyters of Brookhaven National Laboratory and Edwin B. Hooper, Jr., of Lawrence Livermore Laboratory, who reviewed this report and offered useful suggestions. I am also grateful to my colleagues at The Rand Corporation: Robert W. Salter for reviewing the report; Simon Kassel for direction, support of, and interest in the project; and Maureen Cote for assistance in accumulating and organizing the Soviet technical data.

CONTENTS

PREFACE .....	iii
SUMMARY .....	v
ACKNOWLEDGMENTS .....	vii
FIGURES .....	xi
GLOSSARY .....	xv
Section	
I. INTRODUCTION .....	1
II. OVERVIEW OF RESEARCH ON SURFACE-PLASMA SOURCES .....	3
USSR Developments .....	3
U.S. Developments .....	5
III. SURFACE PLASMA ION SOURCES .....	8
Design and Operation .....	8
Basic Design Types .....	10
Principal Operating Characteristics .....	21
IV. OTHER TYPES OF NEGATIVE ION SOURCES AND THE FORMATION OF NEUTRALS .....	27
PIG-Type Sources and DC H <sup>-</sup> Beams .....	27
Charge Exchange Sources .....	29
Formation of Neutrals by Electron Stripping .....	32
V. SPACE CHARGE NEUTRALIZATION OF NEGATIVE ION BEAMS .....	36
VI. CONCLUSIONS .....	54
REFERENCES .....	59

FORCING PAGE BLANK-NOT FILLED

FIGURES

1. Planotron-geometry discharge chamber .....	11
2. $H^-$ ion beam current density in 0.4-mm-wide slit as function of arc current .....	12
3. Planotron-geometry source with elongated emission slit .....	13
4. Dependence of $I_{H^-}$ and $I_T$ on $I_a$ .....	15
5. Semiplanotron surface-plasma negative ion source .....	16
6. Dependence of $H^-$ and $D^-$ ion beam outputs as function of discharge current; emission slit area is noted to right of each curve .....	17
7. Hollow beam negative ion source .....	19
8. Magnetic field intensity between magnetic system poles, with currents in magnetic field coil of 0.5 A (curve 1) and 1 A (curve 2) .....	20
9. Total beam current and negative ion current as function of arc current .....	21
10. Time dependence of hydrogen gas flow and discharge current in a surface-plasma ion source .....	22
11. Discharge voltage in different modes of source operation ....	24
12. PIG-type ion source developed at IFANU .....	27
13. Beam current oscillation coefficient $\kappa$ as function of source hydrogen gas pressure .....	28
14. Conversion coefficient of $H^-$ ions into $H^0$ in gas (Li, Mg, $H_2$ ) and plasma ( $H^+ + e^-$ , $Li^+ + e^-$ , $Mg^+ + e^-$ ) targets .....	32
15. Electron detachment cross sections for $H^-$ ions ( $\sigma_{-10}$ ) and $H^0$ atoms ( $\sigma_{01}$ ) in $H^+ + e^-$ plasma on ions $\sigma^i$ and on cold electrons $\sigma^e$ .....	32
16. Conversion coefficients for hydrogen ions into neutrals in gas targets (solid lines) and plasma targets (broken lines) for 1-- $H_1^+$ ; 2-- $H_2^+$ and $H_3^+$ ; and 3-- $H^-$ .....	33

17.	Dependence of electron capture cross section ( $\sigma_{10}$ , $\sigma_{0-1}$ , $\sigma_{1-1}$ ) and electron detachment cross section ( $\sigma_{-10}$ , $\sigma_{01}$ , $\sigma_{-11}$ ) of hydrogen ions and atoms in molecular hydrogen, $\sigma_{H_0}^H$ is electron capture cross section by hydrogen ions in atomic hydrogen .....	33
18.	Efficiency of deuterium beam injector as a function of energy .....	34
19.	Scattering angle and charge exchange coefficient as functions of target thickness .....	35
20.	Radial potential distribution of negative ion beam .....	37
21.	Radial potential distribution of positive ion beam with and without neutralization .....	37
22.	Beam potential (curve 1) and power density (curve 2) along beam axis as function of Ar pressure .....	38
23.	Potential distribution (curve 1) and negative ion current density (curve 2) as function of chamber width .....	39
24.	Apparatus for beam neutralization experiments .....	39
25.	Potential at beam center as function of background gas pressure .....	40
26.	Radial potential distribution as function of pressure .....	41
27.	Negative ion current density at beam center as function of Kr gas pressure .....	41
28.	Beam voltage change as function of current density .....	42
29.	Current density of alternating beam $J^{\sim}$ (curve 1) and constant beam $J^-$ (curve 2) as functions of voltage amplitude $U_1$ of modulating generator; dependence of $J^-$ on constant voltage applied to modulator (curve 3) .....	44
30.	Radial distribution of beam current density without external modulation (curve 1) and with optimum modulation (curve 2) .....	44
31.	Frequency (curve 1) and amplitude (curve 2) of ion oscillations as functions of air pressure where $H^-$ beam current = 2 mA at 20 keV .....	45
32.	Apparatus for high current density negative ion beam transport .....	47

33. Oscillograms showing beam potential as function of  $z$  with  
 $p = 2.5 \times 10^{-6}$  Torr (slow scan on left, fast scan on  
right) ..... 48
34. Oscillograms showing beam potential as function of  
pressure with  $z = 50$  cm (slow scan on left, fast scan  
on right) ..... 49
35. Radial positive ion current ( $I_+$ ) as function of background  
pressure along beam line at  $z = 18$  cm (curve 1) and  
 $z = 38$  cm (curve 2) ..... 51

GLOSSARY

<u>Ion Source Parameters</u>	<u>Symbol</u>	<u>Units</u>
Negative ion beam current (unspecified)	$I_-$	mA, A
Negative hydrogen ion beam current	$I_H^-$	mA, A
Negative ion beam current density (unspecified)	$J_-$	mA/cm <sup>2</sup> , A/cm <sup>2</sup>
Negative hydrogen ion beam current density	$J_H^-$	mA/cm <sup>2</sup> , A/cm <sup>2</sup>
Arc discharge current	$I_a$	A
Arc discharge voltage	$V_a$	V
Electron beam current	$I_e$	mA, A
Total beam current (total extractor power supply load current) $I_T = I_- + I_e$	$I_T$	mA, A
Extractor voltage	$V_{ext}$	kV
Cathode current density	$W_k$	kW/cm <sup>2</sup>
Source magnetic field	B (or H)	kG (or kOe)
Source discharge chamber pressure	p	Torr, microns
Minimum source pressure to maintain discharge	$P_{min}$	Torr, microns
Neutral gas flow (through emission slit without discharge)	$Q_0$	atoms/cm <sup>2</sup> -s
Gas flow (through emission slit with discharge present)	$Q_a$	atoms/cm <sup>2</sup> -s
Source gas efficiency	$I_-/Q_0$	
Ion source anode aperture (or emission slit) size	A	mm <sup>2</sup> , cm <sup>2</sup>

REPRODUCED PAGE BLANK-NOT FILLED

<u>Ion Source Parameters</u>	<u>Symbol</u>	<u>Units</u>
Normalized beam emittance		
across the emission slit	$E_{nx}$	cm-mrad
along the emission slit	$E_{ny}$	cm-mrad
Normalized beam brightness	$\beta$	A/cm <sup>2</sup> -rad <sup>2</sup>
Beam energy spread	$\epsilon$	eV
<u>Beam Parameters</u>		
Ion beam energy	$E$	keV
Ion beam velocity	$v_b$	cm/s
Ion beam potential	$\phi$	V
Ion beam power density	$W$	W/cm <sup>2</sup>
Distance along beam path (unless otherwise specified measured from ion source anode aperture)	$z$	cm
Full length of the beam trajectory	$L$	cm
Ion beam radius	$r$	cm
Radial positive ion current	$I_+$	mA
Pulsed beam neutralization time	$\tau_n$	$\mu$ s
Background gas pressure at point where $\phi$ changes polarity	$p_0$	Torr
Concentration of atoms in vacuum chamber	$n_a$	
Concentration of atoms in vacuum chamber at pressure $p_0$	$n_{a0}$	
Electron concentration	$n_e$	
Positive ion concentration	$n_+$	

<u>Beam Parameters</u>	<u>Symbol</u>	<u>Units</u>
Negative ion concentration	$n_-$	
Conversion coefficient (positive to negative ion)	$\eta^-$	percent
Conversion coefficient (positive and negative ions to neutral atoms)	$\eta^0$	percent
Gas target thickness	$\delta$	atoms/cm <sup>2</sup> , mol/cm <sup>2</sup>
Electron detachment cross sections		
for $H^-$ to $H^0$	$\sigma_{-10}$	cm <sup>2</sup> /part
for $H^0$ to $H^+$	$\sigma_{01}$	cm <sup>2</sup> /part
for $H^-$ to $H^+$	$\sigma_{-11}$	cm <sup>2</sup> /part
Electron capture cross sections		
for $H^+$ to $H^0$	$\sigma_{10}$	cm <sup>2</sup> /part
for $H^0$ to $H^-$	$\sigma_{0-1}$	cm <sup>2</sup> /part
for $H^+$ to $H^-$	$\sigma_{1-1}$	cm <sup>2</sup> /part
Ionization cross section of gas (formation of gas ions due to collision of negative ions with gas atoms)	$\sigma_i$	cm <sup>2</sup> /part
Electron formation cross section ( $\sigma_e = \sigma_i + \sigma_{-10}$ )	$\sigma_e$	cm <sup>2</sup> /part



## I. INTRODUCTION

This report examines Soviet research on (1) high-intensity, high-brightness negative ion sources and (2) space-charge neutralization, beam transport, and focusing conditions of high-intensity negative ion beams. It also correlates Soviet technical research with data on the Soviet facilities and organizations responsible for ion beam source development.

The Soviets have stated in their research papers that high-current negative ion beams have been developed to create intense neutral beams for injection systems for mirror traps and tokamaks and for inertial confinement fusion. These applications require high-performance characteristics of the neutral beams, particularly high beam current and good beam quality. The same characteristics are required of neutral beams for exoatmospheric beam weapon applications. The present analysis may thus provide insight into Soviet capability to develop such weapons.

This report concentrates on negative ion beams, because they exhibit much higher power efficiencies than positive ion beams in conversion to neutral beams above 200 keV. It examines, in particular, Soviet development of the surface-plasma ion source and includes, for purposes of comparison, a brief account of corresponding U.S. developments. The surface-plasma ion source is currently superior to any other type of ion source presently available in its ability to provide the highest brightness negative ion yields. Since its creation at the Nuclear Physics Institute (NPI) in Novosibirsk in 1971, the surface-plasma ion source has become popular among both Soviet and U.S. researchers and has undergone many modifications and improvements. The source, which has been under continuous development at NPI, has recently received some attention at the Yefremov Institute of Electrophysical Equipment (EFA) in Leningrad and is being applied for negative ion beam transport research at the Physics Institute (IFANU) in Kiev. In the United States, surface-plasma ion sources have been developed at the Brookhaven National Laboratory (BNL), Los Alamos Scientific

Laboratory (LASL), Fermi National Accelerator Laboratory (Fermilab), and Argonne National Laboratory (ANL).

In addition to the surface-plasma ion sources, this report mentions Soviet developments in charge-exchange,<sup>\*</sup> hollow discharge duoplasmatron (HDD), and Penning ionization gauge (PIG) sources. These sources, although of lower brightness, are still of interest in producing negative ion beams. Charge-exchange ion sources have been developed at NPI, the Kurchatov Energy Institute, and the Solid State Physics Institute (IFTT) in Moscow. The HDD source was first developed at EFA following intensive work on duoplasmatrons. Because of its low ion output, the HDD is not extensively covered in this report. PIG-type sources have been used at IFANU in beam transport studies. The remaining ion source types (such as the regular duoplasmatron) have significantly lower output and are, therefore, not included in this report.

---

<sup>\*</sup>Soviet development of charge-exchange sources, especially for neutral beam production, will be discussed in a future Rand report.

## II. OVERVIEW OF RESEARCH ON SURFACE-PLASMA SOURCES

### USSR DEVELOPMENTS

The surface-plasma ion source, known as the magnetron ion source in the United States, was developed in the USSR in the planotron-geometry and Penning-discharge-geometry versions. Of the two, the planotron remains the more efficient in terms of total negative ion yield. The planotron uses an oval cathode surrounded by an anode and operates with the magnetic field parallel to the cathode surface; it can be converted into a Penning-discharge chamber by removing the oval cathode. The planotron can be scaled up in two dimensions; the Penning-geometry source, in only one dimension (by lengthening the cathodes). Recent improvements of the planotron include increased ion yield and gas and power efficiencies.

In the original planotron surface-plasma ion source, developed by Soviet researchers in 1971-1972, the beam current density was increased from 0.75 to 3.7 A/cm<sup>2</sup> by adding cesium vapor to the hydrogen gas in the discharge chamber, producing a maximum of 300 mA of H<sup>-</sup> ions. The source was further developed in 1973 primarily by increasing the length of the emission slit and the associated discharge chamber dimensions. The total H<sup>-</sup> ion yield was increased to 880 mA with an electron beam current of 1.7 A. Without cesium in the discharge chamber, this new version of the source yielded only 15 mA of H<sup>-</sup>.

From 1974 through 1977, the Soviets investigated multiaperture beam-forming systems to raise the negative ion outputs. In the pulsed mode approximately 1 A per cm of slit length was obtained from a planotron-geometry surface-plasma source through a sectional emission slit 3 mm wide. An independent negative ion emitter having a high current discharge with electron oscillations was installed in the discharge chamber. The yield from the source was found to be proportional to the discharge current and the area of the emission slit and was found to be optimum at short gaps between the negative ion emitter and the discharge column. With an emission slit of 0.37 by 10 mm<sup>2</sup>,

the emission current density from the source reached  $5.4 \text{ A/cm}^2$ , a factor of 1.5 higher than that previously obtained from surface-plasma sources.

In 1978, the Soviets developed the semiplanotron surface-plasma ion source. Because it confined the discharge close to the emission slit, the new source required less than half the power previously needed to support the gas discharge. This source yielded 0.9 A of  $\text{H}^-$  and 0.55 A of  $\text{D}^-$  at repetition rates up to 10 Hz. A recent modification of the electrodes of the planotron geometry ion source provided an important means of controlling the discharge, thereby optimizing the source gas and power efficiencies.

A hollow-beam surface plasma source developed in 1978 maintained a symmetric hollow discharge 8 cm in diameter in the pressure range of 0.1 to 1 Torr and formed a hollow beam with a projected maximum beam current of 3 A. The maximum beam output has not yet been reported, but preliminary tests showed positive results with current densities of  $0.7 \text{ A/cm}^2$  for normal operation and  $1.2 \text{ A/cm}^2$  as a maximum.

Gas-flow efficiency measurements made in 1980 on the surface-plasma sources revealed a gas-blocking mechanism. This mechanism, which occurs when the plasma is sustained at the emission slit, can reduce unwanted flows of hydrogen and cesium and is even more effective when continuous or long-pulsed beams are used.

In the Penning-geometry source, discharge voltage and current fluctuations, measured in 1977-1979, demonstrated the presence of a wide range of frequencies. These fluctuations strongly degrade the optics of the output ion beams. However, operations with higher hydrogen gas pressures and weaker magnetic fields eliminated these random fluctuations (noise). Operation in this mode increased the source brightness by a factor of 100 and decreased the beam emittance by a factor of more than 10.

A 100-mA (150-mA max)  $\text{H}^-$  Penning-geometry surface-plasma ion source, produced in 1977, had repetition rates up to 100 Hz and pulse lengths of 300  $\mu\text{s}$ . This source can also be operated in a noiseless mode.

The normalized beam brightness for a Penning-geometry surface-plasma source was found to be  $1$  to  $5 \times 10^6$  A/cm<sup>2</sup>-rad<sup>2</sup> for the noisy and  $10^8$  A/cm<sup>2</sup>-rad<sup>2</sup> for the noiseless operation of the source. The normalized emittance values for the noisy source operation yielded  $E_{nx} = 0.05$  cm-mrad and  $E_{ny} = 0.2$  cm-mrad with energy spread of 1.5 keV and 80 eV, respectively. When the source discharge was adjusted by increasing the source pressure and decreasing the source magnetic field to remove the random fluctuations, the source operated in a noiseless mode and the emittance was reduced to  $E_{nx} = .003$  cm-mrad and  $E_{ny} = .02$  cm-mrad with energy spread of 5 eV and 1 eV, respectively.

Recent Soviet research concentrated on developing a high-current DC and long-pulse-length  $H^-$  and  $D^-$  ion beam by using a modified planotron, a double charge exchange, and a PIG-type ion source. Researchers at the Nuclear Physics Institute (NPI), using a modified planotron geometry source, were reported to have produced an  $H^-$  DC ion beam with a beam current greater than 100 mA in late 1979 [1]. However, this development has not yet been reported in the open literature. In 1980, the Kiev Physics Institute (IFANU) group, using a PIG-type ion source, obtained a 20-mA  $H^-$  DC beam with very low beam current oscillations. In 1977, researchers at Kurchatov Institute, using a charge exchange ion source on the institute's MIN test facility, obtained 1.4 A of  $H^-$  beam pulsed at 10 ms.

In the early 1970s, Yefremov Electrophysical Equipment Institute (EFA) developed the hollow discharge duoplasmatron (HDD), which yielded 6 mA of  $H^-$  (at that time a factor of 3 higher than any previous yield from a standard duoplasmatron source). The development was an outgrowth of concentrated work on duoplasmatrons during the late 1960s. At first, the HDD source's relatively high brightness made it attractive for use in high energy accelerators. However, the HDD's very low power efficiency, the difficulty of removing electrons from the beam, and the relatively low ion yields made it inferior to the surface-plasma source for applications in neutral beam production.

#### U.S. DEVELOPMENTS

The surface-plasma ion source has recently excited much interest and developmental effort in the United States. At present, Brookhaven

National Laboratory (BNL) has an intensive program aimed at producing a 1-A  $H^-$  ion source operational in a steady state (DC) mode or with long pulses (5 to 30 s). Future efforts will be concentrated on a 10-A  $H^-$  source with a cathode power density of 0.1 kW/cm<sup>2</sup> at a cathode current density of about 1 A/cm<sup>2</sup> [2]. BNL has reproduced and further developed the Penning and the planotron geometry surface plasma source as a source for high-energy neutral beams [2-9]. Currents in excess of 1 A of  $H^-$  have been obtained from the planotron geometry magnetron with pulse lengths of 20 ms at a low repetition rate. According to K. Prelec the effort has switched exclusively to the planotron source because of its higher output [6].

BNL achieved a breakthrough in this line of research by developing an asymmetric geometry planotron source with focusing cathodes which increase the gas efficiency by allowing a lower operational discharge gas pressure. The power efficiency was improved by a factor of 3 or 4 to 8 kW/A, while the gas efficiency was increased to about 6 percent. The ratio of electrons to  $H^-$  ions was found to be as low as 0.5 [7]. The latest experiments, using the asymmetric magnetron with focusing grooves in the cathode, demonstrated a decrease in emittance of a factor of 3 [8]. Plans are being made to develop a modified version of the magnetron with plasma injection from a hollow cathode discharge [9]. This research is closely linked to the semi-planotron work performed at NPI. However, the BNL group attempts to operate the source at much lower power densities than those used by NPI in the semiplanotron.

Using NPI (Dudnikov) data, in 1977, P. Allison constructed a Penning-discharge surface plasma source at the Los Alamos Scientific Laboratory (LASL) [10,11]. Over 100 mA of  $H^-$  was obtained with a 750- $\mu$ s pulse length and a repetition rate of 11 Hz; 2 mA was obtained at continuous operation of the source. The U.S. model's emittance generally measured higher than that of the NPI model. LASL expects to decrease emittance measurements by reducing focusing aberrations and noise in the beams.

Researchers at LASL recently obtained up to 160 mA of  $H^-$  extracted at 20 kV from a Penning surface-plasma source with a current density

of  $3.2 \text{ A/cm}^2$  at the extractor [12]. The same researchers, using a circular emission aperture and extractor in their source, observed emittance as a function of beam fraction and found a factor-of-3 reduction in emittance obtained with relatively noise-free discharge voltages [13]. Under optimum conditions, the normalized emittance was measured to be  $0.005 (\pi\text{-cm-mrad})$ .

Research at LASL now also involves the development of a 100-mA DC  $\text{H}^-$  ion source of the Penning geometry with rotating electrodes [14]. In this source, the power density on the electrodes is reduced by magnetically confining the discharge to a small region near the emission aperture. The rotating source, using a fixed anode and rotating cathodes in order to dissipate the power, shows beam outputs and emittances comparable to the fixed-electrode source previously tested.

In 1977, following the LASL drawings, J. Fasolo built a source at the Argonne National Laboratory similar to Allison's first model, to be used on the ZGS accelerator [15,16]. This source operated essentially as the one at LASL and yielded an 80-mA  $\text{H}^-$  beam current. Lower current operation ranged from 30 to 40 mA, with a 500- $\mu\text{s}$  pulse length and repetition rate of 40 Hz.

In the early 1970s, an early version of the BNL source was taken to the Fermilab, where a later model evolved into the Fermilab negative ion source [17]. Developed by Schmidt and Curtis [18,19,20], it now produces 50 mA of  $\text{H}^-$  ions at 750 kV, with a 60- $\mu\text{s}$  pulse length and a repetition rate of 15 Hz. This source, now being used on the Fermilab Linac [21] for  $\text{H}^-$  operation, is reported to have operated dependably for over two years and to have "become the principal ion source for all modes of accelerator operation at Fermilab" [17].

K. Ehlers at the Lawrence Berkeley Laboratory (LBL), using  $\text{H}^-$  ion sources of a different geometry, obtained a 0.5-A  $\text{H}^-$  DC beam (also  $\text{D}^-$ ) from a surface conversion plasma source, using a cusp-shaped magnetic field around the plasma discharge [22]. The negative ions were extracted radially across the magnetic field through a 4 by 10  $\text{cm}^2$  exit aperture. Initial results of Ehler's research are presented in [23] with more recent developments given in [24,25]. Ehler's source is also under consideration for producing neutral beams for injection into tokamaks.

### III. SURFACE-PLASMA ION SOURCES

#### DESIGN AND OPERATION

In 1971, researchers at the Nuclear Physics Institute, while investigating negative ion emission from high-current discharges, discovered a marked increase in  $H^-$  ion emission when cesium was added to the gas discharge [26,27]. These findings led to the development of the surface-plasma method of producing large beams of negative ions and to the subsequent development of the surface-plasma ion source [28,29]. The basic mechanism of surface-plasma negative ion production was described more recently by NPI researchers [30,31,32].

The surface-plasma ion source, so called because of the interaction of the plasma with the electrode surface which results in the formation of negative ions, possesses an oval-shaped cathode surrounded by an anode operating in a magnetic field parallel to the cathode surface. In the presence of a magnetic field, a dense plasma is created in the anode-cathode gap when hydrogen gas is introduced into, and voltage is applied across, the gap. The positive ion bombardment of the cathode forms  $H^-$  ions [33]. Each positive ion acquires two electrons as either (1) it strikes the cathode surface and then is reflected as a negative ion or (2) it sputters atoms from the cathode causing negative ion production. The introduction of cesium into the source and the subsequent coating of the cathode surface lowers the surface electron work function and thus increases the probability of electron capture from the cathode [31].

The negative ions which are thus formed are then accelerated by the cathode potential drop and are passed through the thin cathode plasma sheath toward the emission aperture. To decrease both the energy spread of the ions in the beam and the flow of the accompanying electrons, an equipotential depression, filled with dissociated discharge gas, is formed in front of the emission aperture. Here the fast negative ions, having a large velocity spread, are transformed into slower ions by resonance charge exchange, and the energetic electrons are trapped along the magnetic field lines at the



surface of the depression. In this way, a plasma consisting of low-velocity negative ions along with the positive ions is formed in front of the emission aperture [29].

The  $H^-$  beam is extracted across the magnetic field through the anode emission slit, which is perpendicular to the magnetic field. This design decreases the output of electrons (which are extracted from the source along with the negative ion beam), decreases the total size of the source, and allows a large change in slit length without changing any other source parameters. An optimum magnetic field configuration provides efficient deflection and collection of the undesirable electrons from the beam path.

In the actual operation of the source, several factors complicate the separation of the electron beam from the negative ion beam: the penetration of the extractor electric field into the emission slit, the secondary emission from the walls, the cesium flow from the source, etc. Oscillations in the discharge can increase as well as decrease the electron flow, which depends on the hydrogen and cesium gas inputs and on the extractor voltage [27]. Under optimum conditions, the total electron current in the extraction region is only 1.5 to 2 times greater than the  $H^-$  ion beam current, but in some adverse instances, it can be as high as 10 to 20 times greater.

The space between the emission slit and the extractor electrode is minimized so as to form beams with a high emission current density, to decrease the negative ion loss in the extraction gap, and to reduce electron formation. These factors have been found to be important in the formation of negative ions because of the high gas density in the gas discharge chamber, the large electron detachment cross sections of negative ions, and the extraction of the accompanying electrons in the extractor gap. Only because of the high emission current density can the gas efficiency of the source remain high. Due to the high value of the electric field, the  $H^-$  ions accelerate to several keV, at which the resonance charge exchange cross section decreases considerably for relatively short distances. However, at the minimized extraction distance, defocusing takes place in the extractor and the divergence of the  $H^-$  beam increases along the magnetic field [34].

The spacing between the emission slit and the extractor electrode is usually from 2 to 2.5 mm for an 0.8-mm wide aperture in the extractor electrode. The extractor voltage can usually be varied up to 30 kV. To maintain a stable and rigid system, the emission slit electrode should be massive and the plates of the extractor electrode should be clamped to the source to obtain optimum cooling. In one of the latest surface-plasma source developments, demineralized water is used under pressurized nucleated boiling conditions to force-cool the electrodes, especially the cathode. A precise alignment of the electrodes is necessary: A misalignment of only 0.1 mm along the axis or an equivalent skewing produces an observable displacement in the  $H^-$  ion beam [34].

#### BASIC DESIGN TYPES

##### Planotron Geometry

NPI developed the first model of the planotron surface-plasma ion source between 1971 and 1972. With cesium vapor in the discharge, a 300 mA  $H^-$  ion beam current was extracted from this source, producing a beam current density of  $3.7 \text{ A/cm}^2$ . Without cesium, the current density was only  $0.75 \text{ A/cm}^2$ . With cesium, the source operated with a 1-ms pulsed 150-A discharge current, repetition rated at 10 Hz, at a voltage of 100 to 150 V.

The first model of the source, shown in Fig. 1, had a planotron-geometry discharge chamber with a cold cathode [26,27]. In Fig. 1, the discharge is confined to a ring gap between the central cathode plate (1) and the anode (4) which surrounds it and incorporates the emission slit (9). The cathode face shields (5) limit the extent of the discharge volume. The hydrogen gas is introduced into the discharge through the channel (3) using a pulsed electromagnetic valve. The  $H^-$  ion beam (11) is extracted through the emission slit (9) in the anode across the magnetic field, which is formed by the poles (6). The electric field required for extraction is provided by the extractor electrode (10). The accompanying electrons (8), which

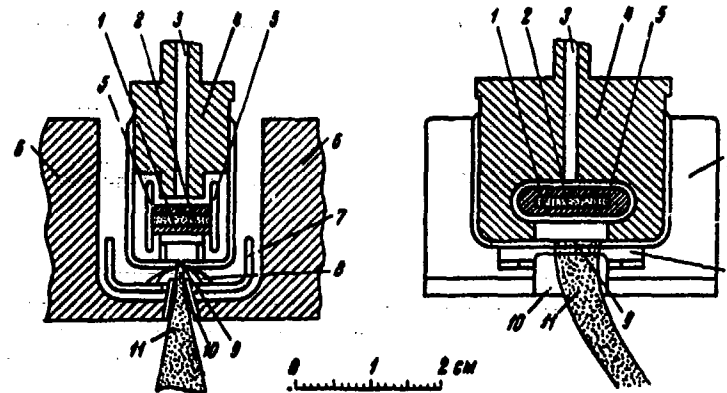


Fig. 1--Planotron-geometry discharge chamber [26]  
(By permission of American Institute of Physics)

- 1--cathode plate
- 2--cathode plate cavity (filled with cesium bichromate and titanium)
- 3--gas inlet channel
- 4--anode
- 5--cathode face shields
- 6--electromagnet poles
- 7--electron collector electrode
- 8--electron beam paths
- 9--emission slit
- 10--extractor electrode
- 11--ion beam

are also extracted from the discharge, are trapped along the magnetic lines of force and are collected on the collector electrode (7).

The cesium vapor is introduced into the discharge chamber when the cathode plate (1), the cavity of which is filled with a mixture of cesium bichromate and titanium (2), is heated by ion bombardment. The density (which must be optimized) of the cesium vapor in the discharge chamber is controlled by the chamber's change in temperature.

The basic parameters required to maintain a normal high-current pulsed discharge in this early version of the source are [26]:

H <sub>2</sub> minimum pressure .....	10 <sup>16</sup> mol/cm <sup>3</sup>
B minimum near cathode .....	1 kG
V <sub>a</sub> (in H <sub>2</sub> + Cs vapor) .....	100 to 150 V
I <sub>a</sub> (1-ms square pulse with repetition rate up to 10 Hz) .....	1 to 150 A

The dependence of  $H^-$  output on the source magnetic field proved to be weak. Any increase in the  $H_2$  pressure in the discharge, above the pressure needed to maintain the arc, decreased the  $H^-$  ion output. The  $H^-$  beam intensity was proportional to the emission slit area over a range of slit width values from 0.4 to 1 mm without cesium and from 0.4 to 2 mm with cesium. The current of the extracted electrons was found to be proportional to the slit length and very strongly dependent on slit width. For a discharge with cesium and a 0.4-mm slit width, the electron current was considerably less than the ion current; with a slit width of 1.5 mm, the two currents extracted were about equal. The maximum  $H^-$  ion beam obtained from this source with cesium in the discharge was 300 mA with a slit of 1 by 10 mm<sup>2</sup>.

The  $H^-$  ion beam current densities developed in a 0.4-mm-wide emission slit at optimum source conditions are shown in Fig. 2 as a function of arc current ( $I_a$ ) with and without the use of cesium vapor in the discharge.

NPI obtained similar discharge characteristics when the source was changed over to a Penning-discharge geometry by removing the cathode plate (1) in Fig. 1. In this case, current densities of 2.5 to 3 A/cm<sup>2</sup> were obtained with cesium in the discharge.

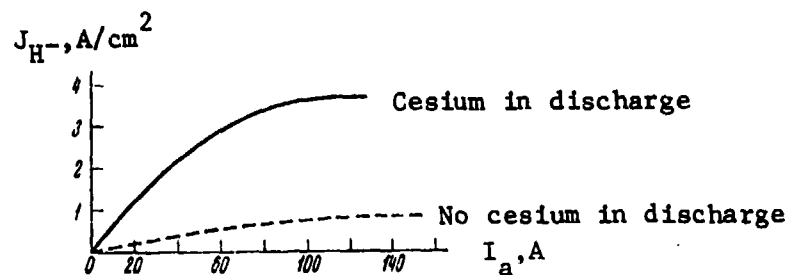


Fig. 2-- $H^-$  ion beam current density in 0.4-mm-wide slit as function of arc current [26]  
(By permission of American Institute of Physics)

#### Revised Planotron Geometry

In 1973, NPI developed a new version of the planotron-type ion source incorporating a longer emission slit (0.9 by 30 mm<sup>2</sup>) and a corresponding longer discharge chamber. This source produced a total

of 880 mA of  $H^-$  ions with an associated electron current of 1.7 A [29]. The maximum current density in the emission slit obtained from this source, shown in Fig. 3, remained  $3.7 \text{ A/cm}^2$  with an emission slit of  $0.4$  by  $5 \text{ mm}^2$ .

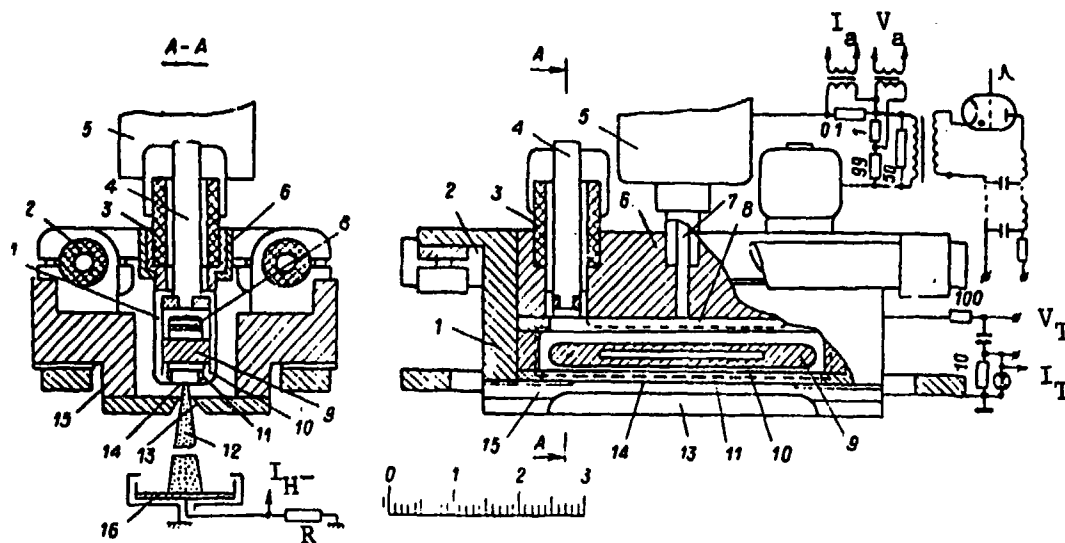


Fig. 3--Planotron-geometry source with elongated emission slit [29]  
(By permission of American Institute of Physics)

- 1--discharge chamber body
- 2--high voltage ceramic insulators
- 3--ceramic cylinder
- 4--support rod for cathode side shields
- 5--fast-acting electromagnet valve
- 6--anode insert
- 7--gas inlet channel
- 8--top anode protrusion
- 9--cathode
- 10--cathode side shields
- 11--bottom anode protrusion
- 12--ion beam
- 13--extractor electrode
- 14--emission slit
- 15--electromagnet poles
- 16--ion beam collector

In Fig. 3, the body of the gas discharge chamber (1) is mounted on high-voltage ceramic insulators (2) between poles (15) of the electromagnet. The discharge chamber, including cathode plate (9), emission slit (14), and extractor electrode (13), is considerably longer than

the source in Fig. 1. Hydrogen gas is fed to the discharge chamber through channel (7) in bursts controlled by fast-acting electromagnet valve (5). The length of each burst can be regulated from  $10^{-4}$  to  $6 \times 10^{-4}$  seconds by changing the parameters of the current pulse opening the valve. The time constant of the gas flow from the discharge chamber through the emission slit is  $10^{-3}$  to  $10^{-2}$  s. This source can maintain pulsed operation with repetition rates up to 10 Hz with a 160 l/s pumping speed beyond the extraction aperture. The cesium was introduced into the discharge in the manner described in connection with the source shown in Fig. 1.

The  $H^-$  beam output was found to be proportional to the area of the emission slit as in the earlier version of the source. In Fig. 4,  $H^-$  beam current ( $I_{H^-}$ ) collected on the Faraday cup and total extractor load current ( $I_T$ ) are plotted as a function of arc current ( $I_a$ ).

The maximum negative ion current output from these sources is observed when the thickness of the cathode plasma layer is at a minimum and the hydrogen gas pressure is sufficiently high to maintain the required arc discharge. Any unnecessary increase in source gas pressure (also the introduction of cesium into the discharge) decreases the negative ion output, because negative ions are easily destroyed at higher gas pressures. With an emission slit of 0.4 by 5 mm<sup>2</sup> and an arc current of 150 A, this source, operating without cesium, yielded 15 mA of  $H^-$ . The corresponding current density was 0.75 A/cm<sup>2</sup>.

In 1975, NPI developed a fast-acting electromagnet valve (item 5 of Fig. 3), allowing pulsed flow of gas with repetition rates up to 1 kHz with an operational life longer than  $10^9$  cycles [35].

A valve developed at EFA in 1978 [36] provides a wide choice of pulse lengths and gas volume adjustments. Using mechanical regulation of the operational gap without disrupting the vacuum, this valve can provide gas flows of  $10^{18}$  to  $10^{23}$  molecules/s at pulse lengths of 0.3 to 2 ms and repetition rates up to 1 kHz. The operational characteristics of the valve did not change for a 100-hour-life test operating at 100-Hz repetition rate. In the case of surface-plasma sources with discharge volumes reaching up to 100 cm<sup>3</sup>, gas flows can be adjusted using this valve to maintain pulsed source pressures of 0.01 to 1 Torr.

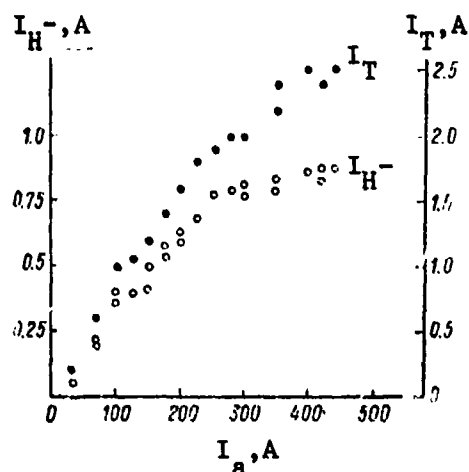


Fig. 4--Dependence of  $I_{H^-}$  and  $I_T$  on  $I_a$  [29]  
 emission slit =  $0.9 \times 30 \text{ mm}^2$   
 cathode =  $4 \times 6 \times 35 \text{ mm}^3$   
 (By permission of American  
 Institute of Physics)

#### Semiplanotron Geometry

In 1978, NPI reported the development of a new version of the surface-plasma ion source in which the discharge, previously confined in the anode-cathode gap, was limited to the area opposite the emission slit [37]. This source, called the semiplanotron surface-plasma source, required only half the power needed to support the gas discharge. The source yielded a maximum of 0.9 A of  $H^-$  and 0.55 A of  $D^-$  at a repetition rate of up to 10 Hz.

The electrode configuration of the semiplanotron is shown in Fig. 5. As in the planotron, the discharge in the semiplanotron is confined in the narrow gap between cathode (1) and the surrounding anode (2). In the semiplanotron, however, the conditions for confinement of fast electrons emitted by the cathode are met only in a small section of the gap near the emission slit (5), which is oriented across the magnetic field. In this area, the magnetic lines are shaped by magnetic inserts (3) to force the electrons to cross the surface of semicylindrical groove (7) in the cathode without touching the anode. This configuration enables the fast electrons to oscillate along the magnetic lines and to be reflected from the cathode. A deep notch (8)

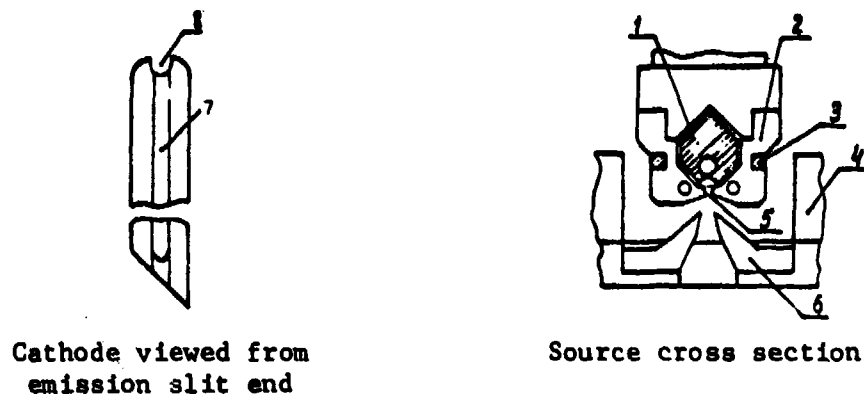


Fig. 5--Semiplanotron surface-plasma negative ion source [37]

- 1--cathode
- 2--gas discharge chamber
- 3--magnetic inserts
- 4--electromagnetic poles
- 5--emission slit
- 6--extractor electrode
- 7--cylindrical groove in cathode
- 8--notch in cathode surface

is made in one side of the cathode to facilitate the striking of the discharge. Bursts of hydrogen gas are fed into this notch by an electromagnetic valve, and cesium is introduced from a heated container. A voltage across the anode-cathode gap in the presence of hydrogen initiates the discharge in the notch. The discharge then spreads along the semicylindrical groove in the cathode adjacent to the emission slit. To eliminate the discharge from other parts of the anode-cathode gap, the cathode and its surrounding anode are shaped to throw the electron in the gap onto the anode along the magnetic lines.

The first experiments with the semiplanotron used an emission slit of 1 by 10 mm<sup>2</sup> located opposite the center of the cathode. The characteristics of the discharge and its dependence on the magnetic field and the hydrogen and cesium input were similar to the characteristics of the planotron chamber discharge in [30]. As the cesium input was increased, the discharge voltage decreased from 400-600 V to 100-150 V, and the H<sup>-</sup> output increased markedly.



The dependence of the  $H^-$  and  $D^-$  beam outputs from the ion source with optimized parameters as a function of discharge current is presented in Fig. 6 for various slit dimensions. When the slit length was increased from 10 to 20 mm, the  $H^-$  and  $D^-$  beam intensity increased by a factor of approximately 2; when the slit length was increased to 40 mm, the proportional beam current increase did not occur. Various slit sizes were tried. The 0.5 by 41 mm<sup>2</sup> slits showed a better homogeneity along the slit than that obtained in the 1 by 40 mm<sup>2</sup> slit and allowed operation at a higher discharge current (up to 150 A). The  $H^-$  beam current reached 0.8 A and  $D^-$  beam current 0.55 A at these settings. When the slit was further increased to 0.72 by 45 mm<sup>2</sup>, the optimum discharge current decreased to 120 A; the  $H^-$  beam output reached a maximum of 0.9 A.

The above experiments with a semiplanotron demonstrated efficient negative ion generation and enhanced beam output with ribbon beam ion sources, using a discharge in crossed fields without a closed electron drift space. An important recent development at NPI, the modification

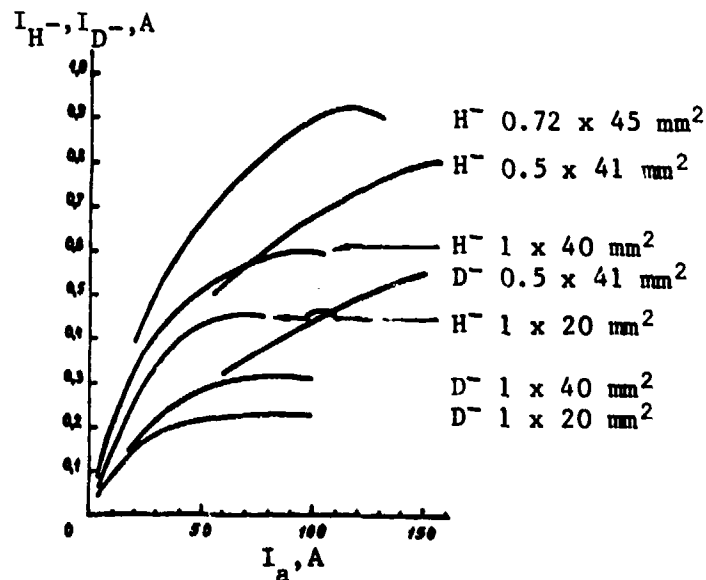


Fig. 6--Dependence of  $H^-$  and  $D^-$  ion beam outputs as function of discharge current; emission slit area is noted to right of each curve [37]

of the planotron-geometry source electrodes (including the development of the semiplanotron), provides better control of the source discharge and optimizes gas and power efficiencies.

#### Hollow-Beam Source

In 1978, Yefremov Electrophysical Equipment Institute in Leningrad (EFA) reported the development of a surface-plasma ion source which generates an axially symmetric hollow  $H^-$  ion beam [38]. This source, which produced current densities of  $0.7 \text{ A/cm}^2$  for normal operation and  $1.2 \text{ A/cm}^2$  as a maximum, had an electron-to-ion beam current ratio of less than 2. EFA investigated various discharge chamber electrode shapes and arrived at a geometry that allowed stable operation and symmetric distribution of the narrow ring channel discharge in the pressure range of 0.1 to 1.0 Torr of hydrogen gas. The emission characteristics were studied as a function of various source parameters; their dependence on the source parameters was found to be similar to that in the normal planotron source. The successful operation of this source indicates the possibility of obtaining 3 A of an  $H^-$  hollow beam with the use of a ring emission slit 1 mm wide. By further optimizing the pressure of the cesium vapor in the discharge and by modifying other elements in the source construction, EFA hopes to achieve larger ion beam outputs.

Figure 7 shows the EFA-designed surface-plasma source intended to produce a high-current axially symmetric  $H^-$  beam. In this source the discharge occurs in crossed E and B fields. The ring electrode geometry of the discharge chamber has an 80-mm anode aperture slit diameter. The toroidal gas discharge chamber of the ion source is formed by a stainless steel anode (1) and cathode (2) located in a radial magnetic field formed by poles (6 and 7) of the magnetic system. The intensity of the magnetic field between the poles of the magnetic system is shown in Fig. 8.

The discharge is held in the ring gap between the anode and the hollow of the cathode. The operating gas is introduced into the discharge chamber (Fig. 7) through the channel (13) located in the cathode support (3) and through twelve 0.8-mm-diameter apertures in the cathode. The cathode has twelve cavities containing pellets (8),

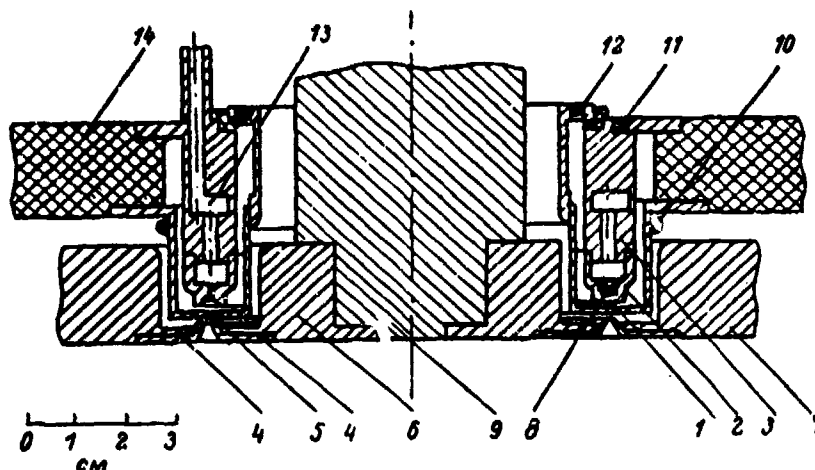


Fig. 7--Hollow beam negative ion source [38]  
(By permission of American Institute of Physics)

- 1--anode
- 2--cathode
- 3--cathode support
- 4--extractor electrode
- 5--anode aperture (emission slit)
- 6 and 7--poles of the magnetic system
- 8--pellets of cesium chromite and titanium mixture
- 9--central magnetic core
- 10--electrode cooling system
- 11--electrode cooling system
- 12--electrode cooling system
- 13--gas input channel
- 14--insulator

made of a mixture of cesium chromite and titanium (30 percent  $\text{Cs}_2\text{CrO}_4$  + 70 percent Ti). The cavities with pellets are covered by metal plates. When the cathode is heated by ion bombardment, cesium is liberated from the pellets and introduced into the gas discharge chamber. The cathode and anode temperatures are regulated by either the cooling system (10, 11, 12) or the power input into the discharge, which, in turn, is controlled by varying pulse frequency from 0.1 to 10 Hz.

The ions are extracted perpendicular to the magnetic field through the anode aperture (in this case the ring slit) by means of the electric field of the extractor electrode (4). The electrons, which are also extracted through the exit slit, are collected at the magnetic field poles along the magnetic field lines.

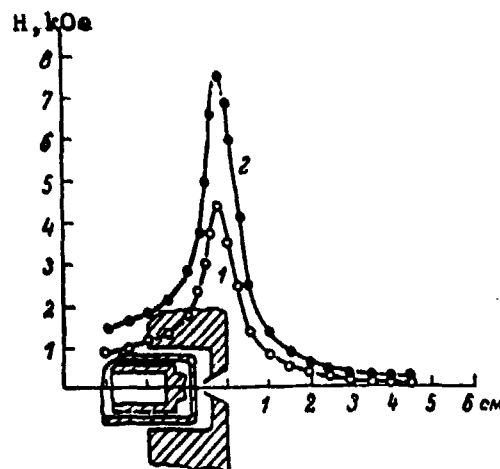


Fig. 8--Magnetic field intensity between magnetic system poles, with currents in magnetic field coil of 0.5 A (curve 1) and 1 A (curve 2) [38] (By permission of American Institute of Physics)

EFA investigated the emission characteristics and the symmetry of the discharge by using six 0.3-mm-diameter apertures (acting as emission apertures) located  $60^\circ$  apart in the anode plates. The maximum negative ion current density under stable source operation-- $0.7 \text{ A/cm}^2$  at a discharge current of 300 A and  $1.2 \text{ A/cm}^2$  at a discharge current of 500 A--occurred just before the ring discharge turned into a nonsymmetric arc. The parameters for optimum ion beam output from the ion source required an arc discharge of 200 V, a magnetic field of 1.2 kgauss, and a hydrogen gas pressure of 0.2 Torr. Various arc discharge currents were tried; unstable source operation was observed at arc currents greater than 300 A. Figure 9 shows the total beam current output ( $I_T$ ) as a function of the arc current ( $I_a$ ). The total beam current consists of the negative ion current ( $I_{H^-}$ ) collected on a Faraday cup, and the accompanying electron current ( $I_e$ ) deflected onto the extractor electrode. In general, the dependence of the ring-geometry surface-plasma source parameters on the source gas pressure, magnetic field, extractor voltage, and arc current is very similar to the dependence found in the planotron-geometry discharge sources.

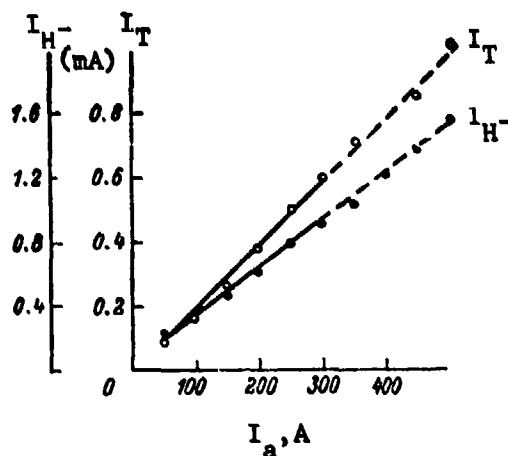


Fig. 9--Total beam current and negative ion current as function of arc current [38] (By permission of American Institute of Physics)

EFA found the best concentration of cesium on the surface of the electrodes to be  $1$  to  $4 \times 10^{14} \text{ cm}^{-2}$ , a value that corresponds to the minimum value of the work function of  $1.2$  to  $1.6 \text{ eV}$  [39]. This concentration is maintained by having the cesium flow onto the chamber surface from a desorption-controlled cesium reservoir. A surface ionization cesium detector was used to study the flow of cesium from the source.

#### PRINCIPAL OPERATING CHARACTERISTICS

##### Gas Flow Efficiency

The Nuclear Physics Institute in Novosibirsk gave special attention in late 1979 to the gas flow efficiency of the surface-plasma sources [40]. Researchers made detailed measurements of the minimum hydrogen gas pressure ( $p_{\min}$ ) required to maintain the discharge in the source and the gas flow out of the source through the emission slit without a discharge ( $Q_0$ ) [28,41]. In a source having a planotron-geometry discharge chamber, the ( $p_{\min}$ ) equals approximately  $0.1 \text{ Torr}$  and the corresponding flow  $Q_0$  is  $20$  to  $30$  times larger than the negative ion output ( $I_{H^-}$ ). The ratio of these two values, namely  $I_{H^-}/Q_0$ , is defined

as the gas flow efficiency and has a value of 3 to 5 percent for surface-plasma sources. NPI's gas-flow measurements showed that the gas flow drops during the source discharge on-cycle [42]. However, noise of the plasma discharge made quantitative analysis impossible.

Using a differential high signal-to-noise ionization counter, NPI measured the gas flow with a discharge present in the source [40]. The time dependence of the various measured signals is shown in the oscillograph trace of Fig. 10. The graph illustrates the drop in the hydrogen flow out of the source during the interval that the discharge is on.

The values of  $Q_0$  represent the hydrogen flow through the emission slit without a discharge in the source;  $I_a$  and  $Q_a$  show the measured values of discharge current and the corresponding hydrogen flow through the slit with the discharge present in the source. The differential signal  $\delta_a$  indicates the noise level caused by the discharge plasma. The discharge is struck when the hydrogen density reaches close to maximum in the region of the farthest anode-cathode gap from emission slit. With an increase in the cesium pressure in the discharge, the values of  $(p_{\min})$  and  $Q_a$  decrease. NPI also determined that with a discharge, the flow of hydrogen through the slit unobstructed by dense plasma actually increases, thereby demonstrating the expulsion of hydrogen from the gas discharge gap.

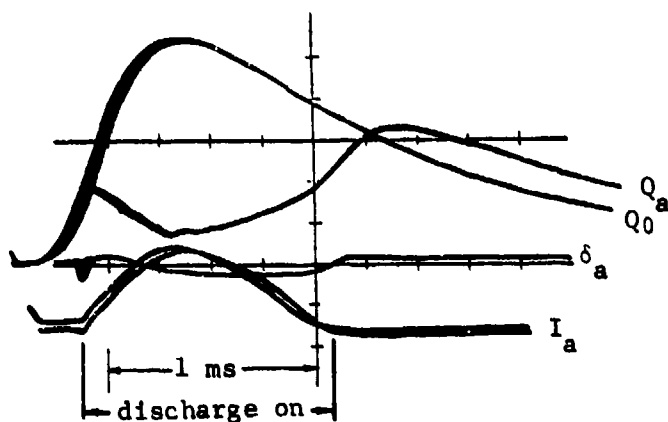


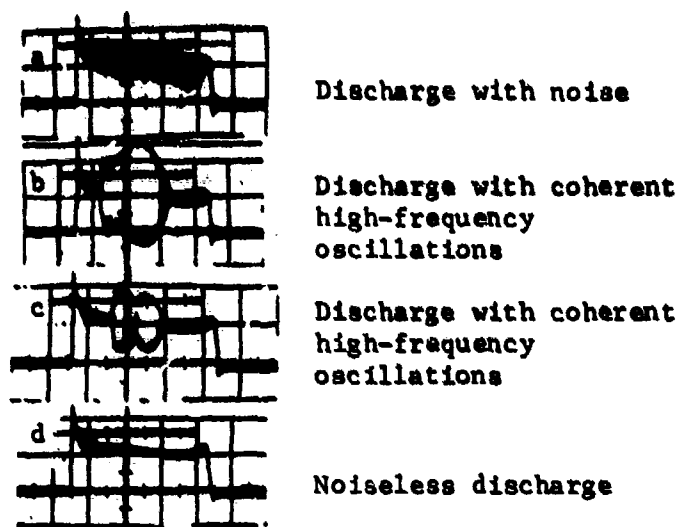
Fig. 10--Time dependence of hydrogen gas flow and discharge current in a surface-plasma ion source [40] (By permission of American Institute of Physics)

The experiments showed that at an optimum cesium concentration, the discharge was struck at  $Q_0 \approx 3$  to  $5 \times 10^{20}$  atoms/cm<sup>2</sup>-s, corresponding to a hydrogen gas pressure  $p \approx 0.1$  to 0.15 Torr in front of the slit. When the discharge current was increased to 50 A, the hydrogen gas flow through the slit ( $Q_a$ ) decreased to  $0.7$  to  $1.0 \times 10^{20}$  atoms/cm<sup>2</sup>-s, with  $p \approx 2$  to  $3 \times 10^{-2}$  Torr, and remained at this level even with an increase in discharge current. Under optimum conditions, the emission of current density ranged from 3 to 4 A/cm<sup>2</sup> ( $2$  to  $2.5 \times 10^{19}$  ions/cm<sup>2</sup>-s), demonstrating that about 30 percent of the total hydrogen gas flow was converted into the  $H^-$  ion beam exiting through the source emission slit. The decrease in hydrogen density near the emission slit decreases the possibility of negative ion loss caused by collisions with background hydrogen gas and guarantees maintenance of high electric strength in the extraction gap region. The gas blocking mechanism in the source caused by the dense plasma as mentioned above and the blocking of cesium as referred to in [39] can be more efficient when continuous DC beams or beams with long pulses are used.

#### Discharge Fluctuations and Noise

NPI observed intense voltage and current fluctuations (noise) in the ion source discharge when it is located in a strong magnetic field. Experiments carried out between 1977 and 1979 showed that these fluctuations degraded the optical properties of the negative ion beams [34, 43,44]. It was determined that the fluctuations could be stopped by decreasing the source magnetic field and increasing the hydrogen and cesium gas pressure. The hydrogen gas pressure had to be increased by a factor of 1.5 over normal operation to stop the fluctuations.

These intense fluctuations, present in most modes of operation in the surface-plasma source with planotron- and Penning-geometry discharge chambers, also appear in HDD sources [34]. Source operation with high noise in the beam, observed at magnetic fields of 1.5 to 2 kG with minimal hydrogen and cesium gas density in the chamber, allowed switching between the glow and the low-voltage discharge mode (100 to 150 V). A typical oscillogram of the discharge voltage in this mode of operation is shown in Fig. 11, a. The frequency spectrum of the



Vertical scale: 100 V/cm  
Horizontal scale: 50  $\mu$ s/cm

Fig. 11--Discharge voltage in different modes of source operation [34]

fluctuations is uniform in the range of 0.1 to 10 MHz. The most effective generation of  $H^-$  ions takes place in this operation mode, but the fluctuations strongly degrade the quality of the output ion beam.

When the source magnetic field is reduced, the fluctuations disappear almost immediately; in certain cases, however, modulated coherent oscillations appear in the frequency range of 17 to 18 MHz (Fig. 11, b and c). The source parameters (magnetic field, discharge current, hydrogen and cesium density) strongly affect the amplitude, but not the frequency, of these oscillations. Further decrease in the magnetic field, or increase in the hydrogen or cesium flow, eliminates the fluctuations of all the discharge parameters (Fig. 11, d). With a fixed geometry of the discharge chamber, the fluctuations disappear at a fixed value of the ratio of the magnetic field to the hydrogen gas density [30]. When the anode slit width is decreased, the criticality of this value increases, i.e., the noiseless discharge is formed at a higher magnetic field and a lower hydrogen density. However, the minimal value of the magnetic field, at which the intense glow discharge is struck, increases, and the operating range of the parameters becomes narrower. The effectiveness of the discharge for the formation of negative ions decreases as slit



width increases. In some modes of operation, high-frequency coherent oscillations (as shown in Fig. 11, b and c) can be generated efficiently; however, the specific nature of such oscillations has not yet been investigated.

In discharges with cesium fluctuations, properties of the cathode can affect noise, which strongly depends on the processes of absorption-desorption of cesium [30,39]. This effect is present at low cesium inputs into the chamber when the cesium concentration changes on the cathode, causing corresponding transition from the low-voltage discharge mode with cesium ( $\approx 100$  V) to the high voltage mode (with voltages up to 1 kV). In discharges without cesium, the noiseless operation is more stable and can be achieved at high magnetic fields (and at higher hydrogen densities). A small amount of cesium can increase the electron scattering and noise damping.

In the noisy mode of operation (Fig. 11, a) there was a correlation between the fluctuation of discharge voltage, discharge current, beam current, and current density. In this case, the normalized beam brightness was 1 to  $5 \times 10^6$  A/cm<sup>2</sup>-rad<sup>2</sup>, and the normalized emittance was 3 to  $5 \times 10^{-2}$  cm-mrad across the slit and 0.1 to 0.2 cm-mrad along the slit, corresponding to the transverse velocity energy spread of 1.5 keV and 0.1 keV, respectively. The beam expanded by a factor of only 2 to 3 in the direction perpendicular to the magnetic field. The factor of emittance difference in the two orthogonal directions was only 3 to 5. The corresponding dimension difference of the emission slit was a factor of 20.

In the discharge mode without noise (Fig. 11, d), the normalized beam brightness was  $10^8$  A/cm<sup>2</sup>-rad<sup>2</sup>, a factor of 100 improvement over the case of the noisy discharge. The minimum normalized beam emittance obtained was  $3 \times 10^{-3}$  cm-mrad across the slit and  $2 \times 10^{-2}$  cm-mrad along the slit.

#### Development of a 100-mA H<sup>-</sup> Ion Source for Accelerators

In 1977, the Nuclear Physics Institute announced the development of a 100-mA H<sup>-</sup> ion source [43] designed for powerful linear accelerators (meson factories) and for circular accelerators with charge-exchange

injection of protons, to be used for proton synchrotron boosters. The source was a new design of a Penning-geometry surface-plasma type with a maximum beam current of 150 mA (100 mA nominal), repetition rate up to 100 Hz, current pulse duration from 100 to 300  $\mu$ s, and ion energy to 30 keV (20 keV nominal).

The discharge volume was filled with hydrogen in 200-ms pulse bursts using the electromagnetic valve mentioned in [35] (see above, p. 14), which has an operational life longer than  $10^9$  cycles. For nominal  $H^-$  ion outputs of 100 mA, the discharge voltage was 100 V, and the total current in the extractor circuit was about 200 mA.

To transport high-current negative ion beams, one must provide either very strong beam focusing or space charge beam neutralization with positive ions. In the beam, ionization of the background gas forms positive ions, and the beam loses negative ions because of electron stripping. Measurements of an  $H^-$  ion beam current at 25 cm from the emission slit showed that 90 to 95 percent of the negative ions were present in the beam at a background pressure of  $5 \times 10^{-5}$  Torr but that only 80 percent were left at a pressure of  $10^{-4}$  Torr. These measurements demonstrate the importance of proper pumping and a control of the background gas pressure for space charge neutralization (see Section V, below).

With the source operating so that the background gas around the beam is well below  $10^{-4}$  Torr and low-frequency fluctuations are present in the discharge, the ion beam diameter at the output increased to 3.5 cm and the normalized beam emittance was 0.04 cm-mrad parallel to the magnetic field and 0.2 cm-mrad perpendicular to the field. When the background gas pressure was increased to  $10^{-4}$  Torr, the beam emittance decreased by a factor of 1.5 to 2 in both directions. In the noiseless mode of operation, the emittance decreased to 0.003 cm-mrad and 0.02 cm-mrad, respectively, and beam diameter was below 1 cm.

#### IV. OTHER TYPES OF NEGATIVE ION SOURCES AND THE FORMATION OF NEUTRALS

##### FIG-TYPE SOURCES AND DC $H^-$ BEAMS

In the investigation of high-current continuous beam (DC) ion sources, 5 mA of  $H^-$  ions was long considered to be the limit of the plasma-discharge-type ion sources [45]. In 1978, IFANU developed a FIG-type ion source which yielded 15 mA of DC  $H^-$  beam with a hydrogen gas flow of 207 cm<sup>3</sup>/min through a 20 by 0.6 cm<sup>2</sup> slit and a discharge current of 3.5 A [46]. The maximum extractable current expected from this source was 40 mA, with an 80-mm slit length and a proportionately larger gas flow. The yield was found to be directly proportional to the neutrals in the discharge chamber and to the emission slit length, but not to the width [47]; see Fig. 12.

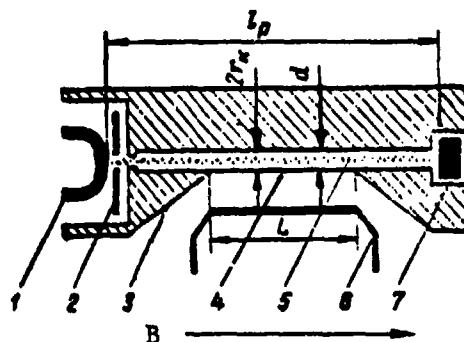


Fig. 12--FIG-type ion source developed at IFANU [46] (By permission of American Institute of Physics)

- 1--tungsten cathode
- 2--tantalum aperture
- 3--anode chamber
- 4--exit aperture in anode
- 5--plasma column
- 6--extractor electrode
- 7--electron reflector

In a 1980 report on (DC) ion sources [48], IFANU disclosed the formation of a 20-mA  $H^-$  ion beam with very low level beam current oscillations. The IFANU team investigated the output of the source for both negative and positive ion beams and compared the beams' oscillations and noise spectra. The dependence of the beam current oscillation coefficient  $\kappa$  on the source hydrogen gas pressure was measured (see Fig. 13). The coefficient for negative ions could be reduced below 0.05 percent at a maximum value of beam current for a range of operating pressures (region B of Fig. 13) and was several orders of magnitude lower than the value for positive ions.

The  $H^-$  ion beam increased linearly with source pressure up to 0.1 Torr, while the  $H^+$  beam was found to depend only weakly on pressure. The maximum beam current of 20 mA  $H^-$  was obtained in this mode of operation with a pressure of 0.1 Torr, a discharge current of 4 A, discharge voltage of 250 V, and an associated electron beam current of 100 mA. The beam noise spectra for both the negative and positive ions in region B were characterized by sharp peaks in the 1-MHz range. The frequency of these peaks decreased as source pressure increased.

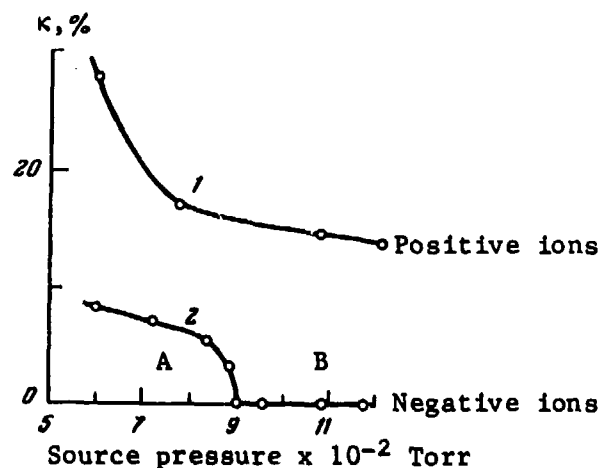


Fig. 13--Beam current oscillation coefficient  $\kappa$  as function of source hydrogen gas pressure [48] (By permission of Plenum Publishing Corporation)

The IFANU team explained [48] the marked difference in beam noise between the negative and positive ions extracted from the source as follows: Fluctuations set up in a plasma discharge having electrons oscillating in a strong magnetic field perturb the plasma column circular profile. This perturbation strongly modulates the positive ion density near the exit slit and the ion beam current. However, all the negative ions leaving the plasma column across its lateral surface, as described in detail in [47], are extracted through the exit slit, so that the beam current is much less sensitive to the fluctuations. This effect is observed in the source operating in region B of Fig. 13.

In 1976, IFANU obtained 1.2 mA of  $\text{Sb}_1^-$  (antimony) ions from the same type of ion source with a current density of 12 mA/cm<sup>2</sup> in the 14 by 0.7 mm<sup>2</sup> emission slit [49]. The associated electron current was 12 mA. The arc discharge was initially struck in Ar (argon); Sb was then introduced from a heated crucible. Subsequently, Ar was cut back to allow optimum operation of the source.

In 1976, IFANU developed a pulsed PIG-type source to produce 80 mA of  $\text{H}^-$  with a pulsed duration of 0.6 ms and a current density of 50 mA/cm<sup>2</sup> at 15 keV beam energy. This source was used to study space charge neutralization of  $\text{H}^-$  ion beam and the self-focusing of the beam, which was observed at relatively high background gas pressures (see below, Section V). Strong beam deneutralization due to beam instabilities was observed at beam current densities of about 50 mA/cm<sup>2</sup> [50].

#### CHARGE EXCHANGE SOURCES

The double charge exchange of a low-energy positive ion beam in various charge exchange targets is another method of producing intense negative ion beams. (An alternate method--the direct extraction from ion sources--is discussed above.) The double charge exchange method is effective in producing large negative ion yields (especially when alkali metal vapor targets are used), but it has a number of major problems: (1) high residual gas pressure along the beam axis; (2) vapor leakage from the charge exchange cell (the leakage contaminates

the vacuum system and degrades the electric strength of the acceleration gaps); (3) the inherently large cross section of the beam; and (4) high beam instabilities.

The Kurchatov Institute in Moscow, Solid State Physics Institute (IFTT) in Chernigolovka, and NPI in Novosibirsk are investigating charge exchange sources. Kurchatov has developed sources and charge exchange targets geared for neutral beam injectors for thermonuclear reactors [51]. In 1976, Kurchatov began operating a special test facility (MIN), built specifically for research on charge exchange systems and negative ion injectors. The facility's power supply capabilities allow positive ion currents of up to 100 A at 10 keV and negative ion currents of up to 10 A at 100 keV, with pulse lengths up to 1.5 s and intervals between pulses of 40 to 60 s [52]. As reported in 1977, MIN obtained  $H^-$  ion beam currents of 1.4 A at 40 keV using an 8-A  $H^+$  beam at 10 keV with a pulse length of 10 ms focused into a Na or Cs vapor target. The negative ion beam formed represented about 18 percent of the total current of positive ions and neutrals channeled through the charge exchange cell. Beams up to 20 A  $H^+$  have been tried, but higher negative ion yields have not been reported. The IBM-5 positive ion source [53], a copy of the Berkeley bucket source used at Kurchatov, is designed for the T-11 tokamak injector, which provides neutral atoms with an energy of 25 keV and a power of 500 kW. This source produces over 30 A of  $H^+$  at 25 keV with a pulse length of 20 ms and uses no external magnetic field. The source's emission aperture, consisting of 42 slits (each 8 by 0.2 cm<sup>2</sup>), provides an initial beam cross section of 8 by 18 cm<sup>2</sup>. The dispersion angle of the beam is  $\leq 0.6^\circ$  along the slits and  $2.5^\circ$  perpendicular to the slits.

At the Solid State Physics Institute (IFTT), a team headed by B. A. D'yachkov conducted work on all aspects of charge exchange. Development of various metal vapor targets for the production of both negative ions and neutrals began in the mid-1960s. The early investigations of an ultrasonic lithium vapor target (and later sodium, magnesium, and zinc vapor targets) for the production negative ions showed that the conversion coefficient ( $\eta^-$ ) for  $H^+$  to  $H^-$  was considerably higher for metal vapors (here Zn and Mg) than for gas targets

[54,55]. This coefficient sharply decreased as a result of an increase in positive ion beam energy. At 20 keV, the coefficient was 2.5 percent for Zn, 1 percent for Mg, and only 0.2 percent for Li and Na. Vapor leakage into the vacuum was studied in [56]. In 1971, a Na vapor target developed for  $\text{He}^-$  production showed a 1.7 percent conversion coefficient at an optimum beam energy of 12 keV [57].

More detailed measurements of the conversion coefficients for  $\text{H}^+$  to  $\text{H}^-$  were also made during 1971 [58]. Optimum values of 5.3 percent for Li, 9.5 percent for Na, 4.2 percent for Mg, and 9 percent for K at 2 keV positive ion-beam energy were obtained. The optimum value of the charge exchange target thickness was  $2 \times 10^{15}$  atoms/cm<sup>2</sup> for alkali metals and  $3 \times 10^{15}$  atoms/cm<sup>2</sup> for Mg. By comparison, the conversion coefficients in gas targets normally run about 2 percent. The conversion coefficients of other ion species were measured in 1975 [59]. The coefficient for  $\text{O}^+$  to  $\text{O}^-$  conversion was found to be about 47 percent in K, 35 percent in Na, 33 percent in Mg, and 22 percent in Cd at 3 keV. In this work the  $\eta^-$  for  $\text{H}^-$  was optimized at 12 percent for a 2.5 keV beam, which is in agreement with NPI's measurements [60].

In 1973, IFTT constructed a Li vapor target with beam line apertures 4.5 cm in diameter and a target thickness of  $5 \times 10^{15}$  atoms/cm<sup>2</sup>; the target thickness could be maintained continuously for 20 hours by circulating and recovering the Li [61]. A Na vapor target with a 10-cm-diameter beam aperture, constructed in 1975, provided the optimum target thickness of 2 to  $3 \times 10^{15}$  atoms/cm<sup>2</sup> for continuous periods of 70 hours [62].

In 1973, the NPI team that developed the surface-plasma ion source produced a pulsed charge exchange ion source [60]. This source, which used a hydrogen-filled charge exchange cell, yielded 54 mA of  $\text{H}^-$  with a pulse length of 100  $\mu\text{s}$ . The normalized emittance of the beam was 0.2 cm-mrad by 0.025 cm-mrad. This source was used on a Van de Graff accelerator, which provided an output of 20 mA of  $\text{H}^-$  at 1 MeV with a pulse length of 200  $\mu\text{s}$  [63]. NPI reported on the work on charge exchange, measurement of conversion coefficients, and electron stripping of negative ions [64], in a 1978 review article [65].

### FORMATION OF NEUTRALS BY ELECTRON STRIPPING

High-energy neutral hydrogen atoms and molecules (or hydrogen isotopes) are most efficiently formed by injecting an  $H^-$  ion beam into gas or plasma targets (i.e., by removing an electron from the  $H^-$  ion or H atom). The effectiveness of this method results from the large cross section for the detachment of one electron from the  $H^-$  ion or H atom. In gas targets, up to 65 percent of the  $H^-$  ions can be converted to hydrogen atoms (Fig. 14) [55,65]. Plasma targets provide even higher values of cross sections, allowing up to 80 to 85 percent of  $H^-$  ions to be converted into neutrals at ion energies greater than 100 keV (Fig. 14) [64,66,67]. The electron detachment cross sections for  $H^-$  ions ( $\sigma_{-10}$ ) and  $H^0$  atoms ( $\sigma_{01}$ ) in an  $H^+ + e^-$  plasma are shown in Fig. 15.

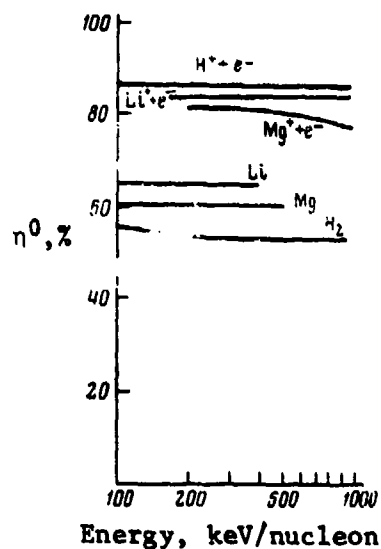


Fig. 14--Conversion coefficient of  $H^-$  ions into  $H^0$  in gas (Li, Mg,  $H_2$ ) and plasma ( $H^+ + e^-$ ,  $Li^+ + e^-$ ,  $Mg^+ + e^-$ ) targets [65]

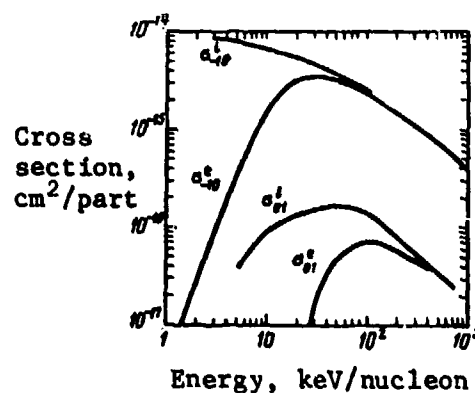


Fig. 15--Electron detachment cross sections for  $H^-$  ions ( $\sigma_{-10}$ ) and  $H^0$  atoms ( $\sigma_{01}$ ) in  $H^+ + e^-$  plasma on ions  $\sigma^i$  and on cold electrons  $\sigma^e$  [65]

(By permission of American Institute of Physics)



In Fig. 16, the efficiency of transforming protons, molecular ions, and  $H^-$  ions into fast neutral atoms is shown at various energies, using optimized gas and plasma targets [65]. The relative inefficiency of neutral hydrogen production from positive ions at energies greater than 100 keV is evident. This inefficiency stems from the drop-off of the cross sections (see Fig. 17). Additional increases in the

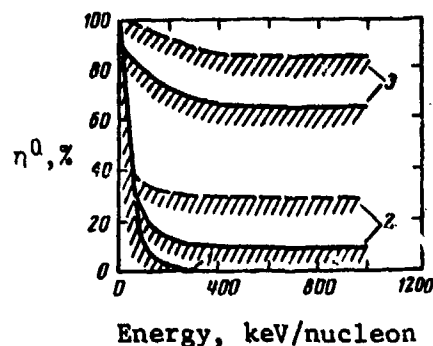


Fig. 16--Conversion coefficients for hydrogen ions into neutrals in gas targets (solid lines) and plasma targets (broken lines) for 1-- $H_1^+$ ; 2-- $H_2^+$  and  $H_3^+$ ; and 3-- $H^-$  [65]

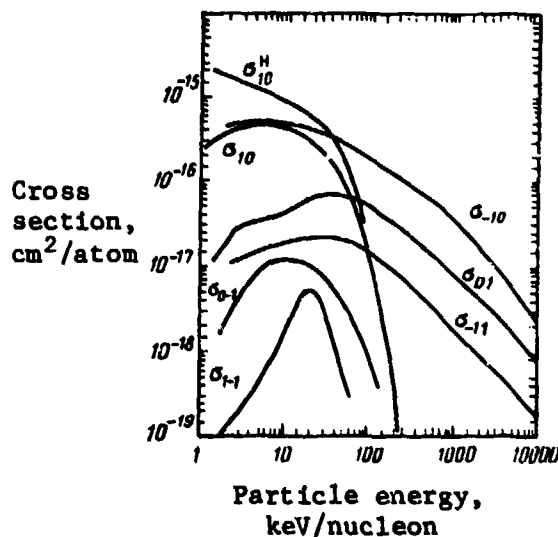


Fig. 17--Dependence of electron capture cross section ( $\sigma_{10}$ ,  $\sigma_{0-1}$ ,  $\sigma_{1-1}$ ) and electron detachment cross section ( $\sigma_{-10}$ ,  $\sigma_{01}$ ,  $\sigma_{-11}$ ) of hydrogen ions and atoms in molecular hydrogen;  $\sigma_{10}^H$  is electron capture cross section by hydrogen ions in atomic hydrogen [65] (Figs. 16 and 17 by permission of American Institute of Physics)

efficiency of neutral hydrogen beam production can be obtained by using photon targets with which the  $H^- \rightarrow H^0$  transformation can be achieved with 100 percent conversion [68,69,70].

In 1980, the Kurchatov Institute, using a double charge exchange ion source, designed a neutral beam injector for thermonuclear reactors to provide deuterium atoms at energies of 400 to 600 keV [51]. Figure 18 shows the efficiency of the neutral beam injector as a function of beam energy for both positive and negative ion beam use. This figure shows again that optimum operation at higher energies is accomplished with negative ions (in this case obtained by charge exchange in cesium and sodium).

Solid State Physics Institute (IFTT) measured the conversion of negative ions of  $C^-$ ,  $O^-$ ,  $F^-$ , and  $Cl^-$  into neutral beams in gases ( $H_2$ , He,  $CO_2$ , air) and metallic vapors (Li, Na, Mg) in [71]. The charge exchange coefficient was measured as a function of energy from 110 to 380 keV; typically the coefficient ranged from 40 to 60 percent in gases, 60 to 70 percent in metal vapors, and 35 to 45 percent in  $CO_2$  at 200 keV.

The scattering angle of neutral hydrogen formed by the electron stripping of  $H^-$  ions at energies of 50 to 150 keV was measured in

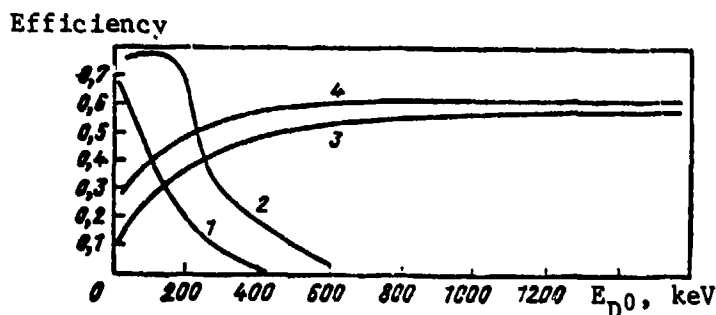


Fig. 18--Efficiency of deuterium beam injector as a function of energy [61] (By permission of Plenum Publishing Corporation)

- 1--positive ion injector
- 2--positive ion injector plus energy recovery (90 percent efficiency)
- 3--negative ion injector (charge exchange in Cs)
- 4--negative ion injector (charge exchange in Na)

H<sub>2</sub>, He, and Li targets for target thickness of  $5 \times 10^{14}$  to  $1 \times 10^{16}$  atoms/cm<sup>2</sup> [72]. The scattering angle of neutrals was found to be independent of target thickness in the normal thickness range. The angle was basically determined by the nonelastic electron stripping process and varied with increase in energy as  $E^{-1/2}$ . The scattering angle and the charge exchange coefficient  $\eta^0$  are shown in Fig. 19 as functions of target thickness and energy for H<sub>2</sub> and He. For comparison, the values for the proton-to-neutral hydrogen conversion, shown by the dashed line, demonstrate inferior operation.

A 1980 NPI paper on the production of neutrals [73] describes experiments using a hydrogen plasma target to convert a D<sup>-</sup> ion beam into neutral deuterium atoms. A stable plasma was set up along magnetic lines of force; the plasma reached a density of  $3 \times 10^{13}$  cm<sup>-3</sup> with a composition of 85 percent H<sup>+</sup> and 15 percent H<sub>2</sub><sup>+</sup>. In preliminary investigations, the plasma target thickness was measured by observing the attenuation of a 5-keV atomic hydrogen beam as the latter passed through an 80-cm length of the plasma. The atomic hydrogen beam was created by the diagnostic injector as described in [74]. For 60 kW and 800-A discharge in the plasma-forming source, the target thickness was determined to be  $2.2 \times 10^{15}$  atoms/cm<sup>2</sup>. This thickness corresponds to the optimum thickness for neutralizing 1 MeV D<sup>-</sup> ions.

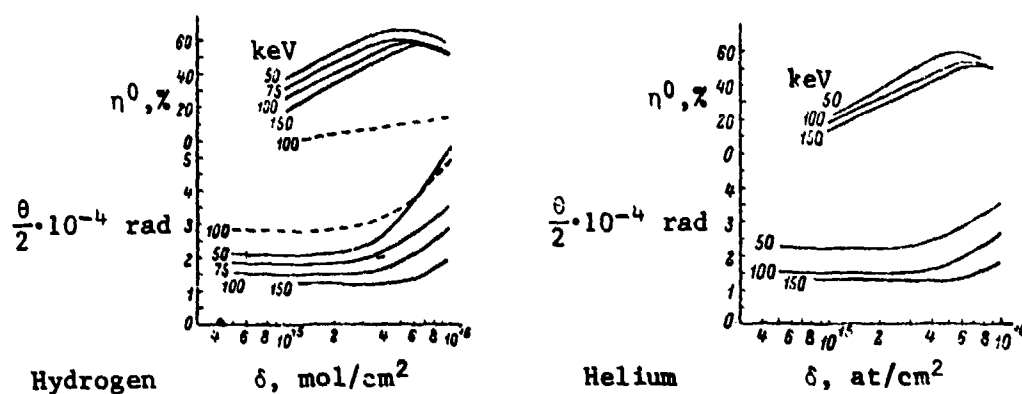


Fig. 19--Scattering angle and charge exchange coefficient as functions of target thickness [72]  
(By permission of American Institute of Physics)

## V. SPACE CHARGE NEUTRALIZATION OF NEGATIVE ION BEAMS

The Physics Institute (IFANU) in Kiev devoted a large effort, headed by M. D. Gabovich, to the study of ion beam space charge neutralization and beam transport and focusing conditions. The investigations, begun in the early 1960s, included space charge neutralization of both positive and negative ion beams, transport and focusing of neutralized ion beams, dynamic deneutralization of beams, and collective oscillations in neutralized ion beams and their effect on ion beam transport.

Investigating space charge neutralization of a high-current negative ion beam in 1973-1974, the Gabovich team observed self-focusing of the ion beam as it passed through gas at a relatively high pressure [75]. In these and later experiments in 1978-1979 [76,50,77,78], the beam potential  $\phi$  was measured as a function of beam parameters and type and pressure of the background gas. The beam potential was found to change with gas pressure and to show a polarity reversal above a certain value of background gas concentration. Coulomb repulsion controlled the beam potential. Repulsion between the ion beam and the plasma electrons transferred enough energy to the electrons to make the latter leave the potential well formed by the space charge of the slow plasma ions. Coulomb repulsion also caused the electron buildup to decrease and allowed the beam neutralization with a positive space charge to compress the beam, thus creating the "gas focusing" condition. In the case of positive ion beams, this mechanism led to deneutralization and defocusing. Unfortunately, gas focusing of the negative ion beam occurred at a relatively high gas pressure, at which the collision of the gas atoms with the negative ions leads to a loss of negative ions by electron detachment. For best beam transport conditions, an optimum pressure must be chosen to allow maximum beam focusing over a long distance without undue beam loss.

The beam potential reversal is illustrated in Fig. 20. The radial potential distribution of a negative ion beam is shown: (a) drifting through a vacuum, (b) passing through gas with a high degree of neutralization, and (c) passing through high-pressure gas

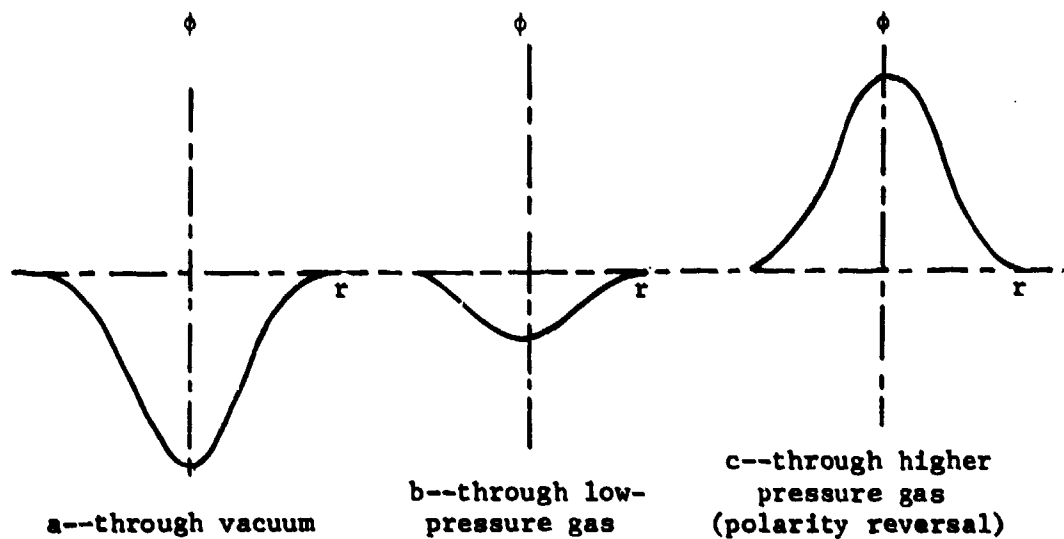


Fig. 20--Radial potential distribution of negative ion beam with a polarity reversal of potential. The potential distribution of a positive ion beam is shown for comparison in Fig. 21.

In their initial research into gas focusing of an  $H^-$  ion beam in 1973, the Gabovich team injected a 10-mA current beam at 10 keV into argon gas at various pressures and, using a thermoprobe, measured

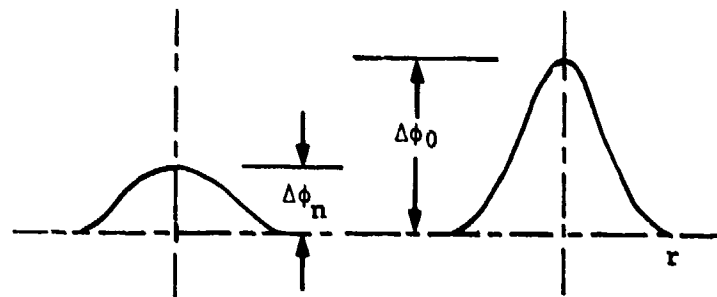


Fig. 21--Radial potential distribution of positive ion beam with and without neutralization

$\Delta\phi_0$ --initial value of potential well

$\Delta\phi_n$ --neutralized value of potential well

the beam potential  $\phi$  along the beam axis at 100 cm from the source [75]. Figure 22, based on the experimental data, shows values of beam potential versus argon gas pressure in the drift chamber.

At pressure  $p_0 > 10^{-4}$  Torr (for argon), the beam potential changes from negative at lower pressures to positive at higher pressures. In addition to the change in beam potential, the probe showed an increase in the power density  $W$  along the axis of the beam (curve 2 in Fig. 22), thereby demonstrating the presence of gas focusing. To examine this effect in more detail, the Gabovich team measured the radial distribution of the beam potential (along the whole width of the chamber at pressures considerably greater than  $p_0$ ) and the corresponding distribution of the beam current density. These measurements, shown in Fig. 23, demonstrate a two-step potential distribution in which the electric field on the beam boundary causes the beam to compress. The distribution does not represent the full potential drop ( $\phi_1 + \phi_2$ ), but only the small potential drop ( $-\phi_2$ ) in the proximity of the beam. The small potential drop and the loss of electrons from the negative ions at the higher pressure range (see the drop of  $W$  in Fig. 22, curve 2) both contribute to the relatively small compression of the beam. Even at  $p_0$ , the mean free path for this process of electron detachment is on the order of the path length of the beam in the gas.

The two-step potential distribution should be seen in the transport of all high-intensity particle beams through gas with a sufficiently

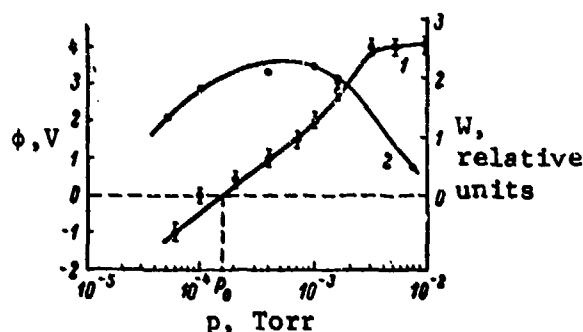


Fig. 22--Beam potential (curve 1) and power density (curve 2) along beam axis as function of Ar pressure [75] (By permission of American Institute of Physics)

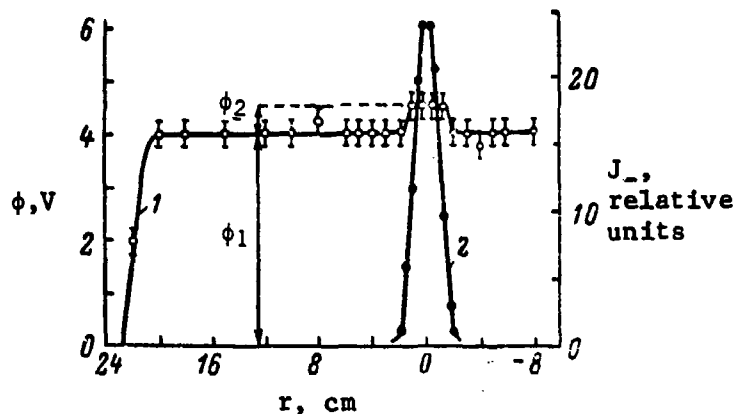


Fig. 23--Potential distribution (curve 1) and negative ion current density (curve 2) as function of chamber width [75] (By permission of American Institute of Physics)

high concentration of atoms. When electrons or negative ions are transported, the electric field at the beam boundary exerts a focusing effect; however, when positive ions are transported, the electric field always defocuses the beam.

The recent experiments on the  $H^-$  ion beam space charge neutralization described in [76] used the setup shown in Fig. 24. The ions were extracted from the ion source (1) perpendicular to the magnetic

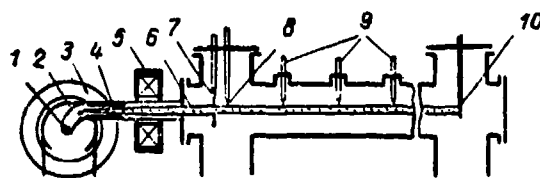


Fig. 24--Apparatus for beam neutralization experiments [76] (By permission of American Institute of Physics)

- 1--negative ion source
- 2--liner
- 3--magnetic field coil
- 4--magnetic shield
- 5--magnetic lens
- 6--beam
- 7--aperture
- 8,9--probes
- 10--target

field produced by the coils (3) of the liner field (2). They entered the magnetic shield (4) and were focused on the target (10) by the lens (5). The maximum beam current  $\approx 6$  mA at 12 keV, with a negative ion concentration of  $n_- = 10^7$  to  $10^8$  cm $^{-3}$ . The radial distribution of the static potentials was measured with thermocouple probes and collectors; voltage oscillations were measured with capacitive probes [79].

The potential at the center of the beam, measured as a function of gas pressure, is shown in Fig. 25. As the pressure increases, the potential changes from a negative to a positive value. The zero value of the potential appears at  $p = 3 \times 10^{-4}$  Torr for helium,  $4 \times 10^{-5}$  Torr for air, and  $2 \times 10^{-5}$  Torr for krypton. The values agree with calculations based on the ion plasma balance equation [76]. The calculated values for zero potential appeared at  $p = 1.1 \times 10^{-3}$  Torr for helium,  $8 \times 10^{-5}$  Torr for air, and  $2.4 \times 10^{-5}$  Torr for krypton, assuming an ion temperature of 0.1 eV and ionization cross sections  $\sigma = 4 \times 10^{-17}$ ,  $2 \times 10^{-16}$ ,  $4 \times 10^{-16}$  cm $^2$ /part, respectively. The beam potential  $\phi$  at low gas pressures does not depend on the type of gas used (see Fig. 25).

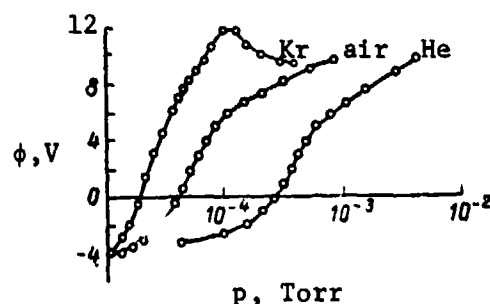


Fig. 25--Potential at beam center as function of background gas pressure [76] (By permission of American Institute of Physics)

$H^-$  beam current  $\approx 3$  mA  
beam energy = 10 keV



The radial beam potential distribution, measured by a thermocouple probe as a function of pressure, is shown in Fig. 26. At low pressures (below approximately  $5 \times 10^{-5}$  Torr), the potential drop takes place within the beam. At higher pressures, when the concentration of the plasma ions is much greater than the concentration of the beam particles, the observed voltage falloff at the beam boundary demonstrates a plasma beyond the limits of the beam.

Ion focusing of the beam was more pronounced in krypton than in air or argon [75]. Figure 27 demonstrates negative ion current density

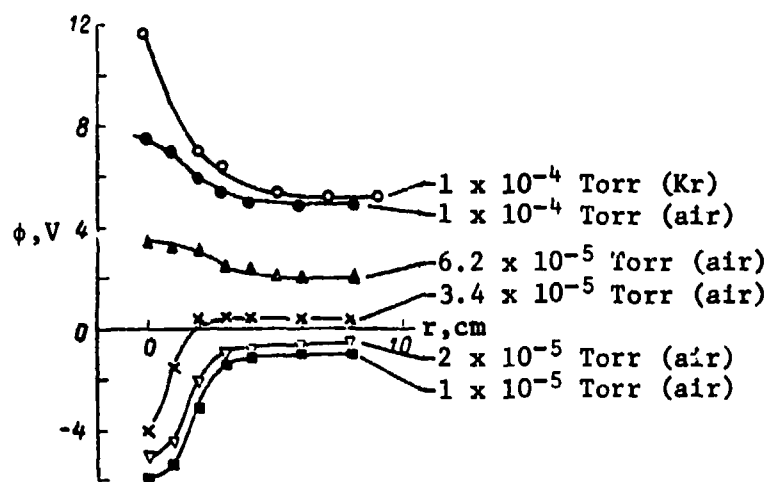


Fig. 26--Radial potential distribution as function of pressure [76] (By permission of American Institute of Physics)

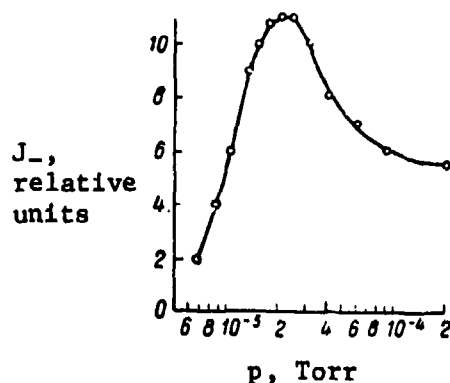


Fig. 27--Negative ion current density at beam center as function of Kr gas pressure [76] (By permission of American Institute of Physics)

as a function of Kr pressure, with the best focus at  $2 \times 10^{-5}$  Torr [76,77].

IFANU compared calculations and measurements of the potential drop  $\Delta\phi$  as a function of beam current density. Figure 28 shows the experimental data, represented by the points, with air pressure at  $1 \times 10^{-4}$  Torr and a beam current of 5 mA at 10 keV. Figure 28 also shows the calculated values for krypton and air for comparison; although the calculations were only approximate, the agreement with the measurements is reasonable. This comparison demonstrates that a relatively high value of  $\Delta\phi$  at  $n_a > n_{a0}$  (where  $n_a$  is the concentration of atoms in the chamber and  $n_{a0}$  is the concentration of atoms at  $p_0$ ; see Fig. 22 above) is achieved by Coulomb repulsion between the beam ions and the electrons. These electrons obtain the necessary energy to leave the potential well formed by the space charge caused by the slow plasma ions.

At high pressures, the scattering of and electron detachment from the negative ions become significant, decreasing the current density (see Fig. 27, above). The distance that the ions can travel without substantial losses in the case of gas focusing is  $l \leq 1/n_a \sigma_{-10}$  (approximately 200 cm in the case of air and krypton). IFANU concluded, therefore, that gas focusing could be used only for short beam transport distances at high pressures.

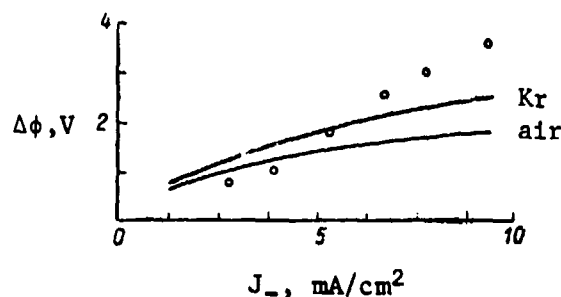


Fig. 28--Beam voltage change as function of current density [76] (By permission of American Institute of Physics)

During beam transport in low background pressures, the values of  $\Delta\phi$  are negative and in a low voltage range (see Fig. 26, above). Analysis has shown that in a stable negative ion beam such high values of beam potential should not exist. Assuming that  $\Delta\phi$  is determined by Coulomb interaction between beam and plasma ions, calculations show that  $\Delta\phi$  should have a value of about  $10^{-2}$  V and that the concentration of the ion beam should be  $n \sim 10^8 \text{ cm}^{-3}$  ( $I \sim 6 \text{ mA}$ ). In the other possible deneutralization mechanism--the recombination of plasma ions with beam ions-- $\Delta\phi$  should be  $\leq 10^{-2}$  V. Thus, the observed value of  $\Delta\phi$  can be assumed to be connected to dynamic deneutralization. Experiments investigating dynamic deneutralization in positive ion beams [80,81] showed that the beam current was modulated with monochromatic oscillations which, depending on the source discharge, varied from 200 to 500 kHz. The amplitude of these oscillations, ranging from 10 to 20 percent of the total negative ion beam current, can cause voltage oscillations which, in turn, can generate beam deneutralization.

From the above experiments and analysis, IFANU reached the following conclusions:

1. The Coulomb repulsion between the ion beam and the plasma electrons determines the value of the positive potential in a negative ion beam passing through a gas of sufficiently high pressure.
2. A suitable selection of gas species can achieve an optimum compression of the beam through gas focusing.
3. Current oscillations tend to deneutralize the beam if the background pressure is not sufficiently high [76].

Experimental investigations in 1974 demonstrated radial focusing of a negative ion beam as the beam passed through and excited ion oscillations in a plasma [82]. Plasma formed by the negative ion beam ionization of the background gas has a small concentration of electrons at low gas pressures. Standing oscillations occur along the beam radius. The whole beam interacts with the plasma ion

oscillations and focuses towards the axis. In experiments made in air at  $p_0 = 5 \times 10^{-5}$  Torr, the beam potential had a value of zero and the loss of negative ions from collisions with background pressure was negligible. Ion oscillations with maximum amplitudes corresponding to the Langmuir ion frequency were induced in the beam without external modulations. The application of an external, large-amplitude signal at this frequency in the beam dampened all (except signal) oscillations. Probe measurements demonstrated that the phase of the oscillations does not change along the beam diameter and that the maximum amplitude is found at the beam axis.

The effects of radial focusing of the beam particles are demonstrated in Figs. 29 and 30. In Fig. 29, the current density along the

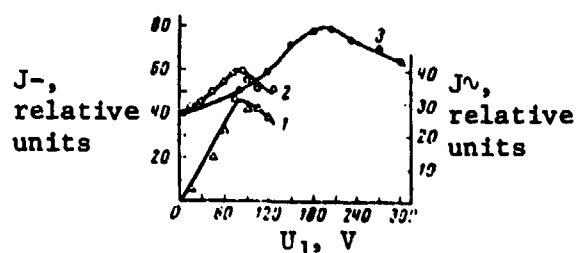


Fig. 29--Current density of alternating beam  $J_v$  (curve 1) and constant beam  $J_-$  (curve 2) as functions of voltage amplitude  $U_1$  of modulating generator; dependence of  $J_-$  on constant voltage applied to modulator (curve 3) [82] (By permission of American Institute of Physics)

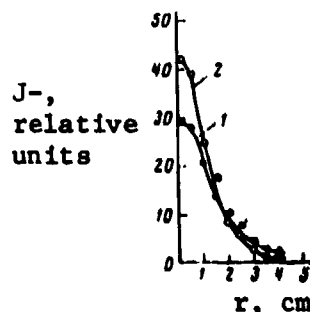


Fig. 30--Radial distribution of beam current density without external modulation (curve 1) and with optimum modulation (curve 2) [82] (By permission of American Institute of Physics)

beam axis for an alternating beam  $J_v$  (curve 1) and a constant beam  $J_-$  (curve 2) are shown as functions of the voltage amplitude of the modulated signal  $U_1$ , which determines the initial amplitude of the radial beam velocity. Measurements were made at a distance of 220 cm from the modulator at a pressure of  $5 \times 10^{-5}$  Torr and a modulating frequency of 140 kHz.

Figure 30 shows the radial distribution of the current density  $J_-$  in the beam without external modulation (curve 1) and with optimum modulation (curve 2), with  $U_1 = 80$  V,  $f = 140$  kHz,  $z = 220$  cm, and  $p = 5 \times 10^{-5}$  Torr. These figures show that the radial ion oscillations of the plasma cause radial focusing of the beam particles; optimum radial focusing occurs at  $z = 220$  cm, with  $V_1 = 4 \times 10^5$  cm/s, figures that agree with calculations made in [83].

IFANU's 1974 research on the collective interaction of a fast negative ion beam with plasma ions demonstrated that even at very low background pressures, low frequency oscillations (the frequency of which increased with pressure [plasma density]) occurred in the system [84]. The frequency and amplitude of these oscillations as functions of pressure are shown in Fig. 31. Damping, caused by the collision of the charged particles with neutrals, leads to an amplitude decrease at higher pressure (as in the case of positive ions [85,86]). Negative ion beams show more pronounced ion oscillation excitation than positive ion beams under much broader gas pressure ranges.

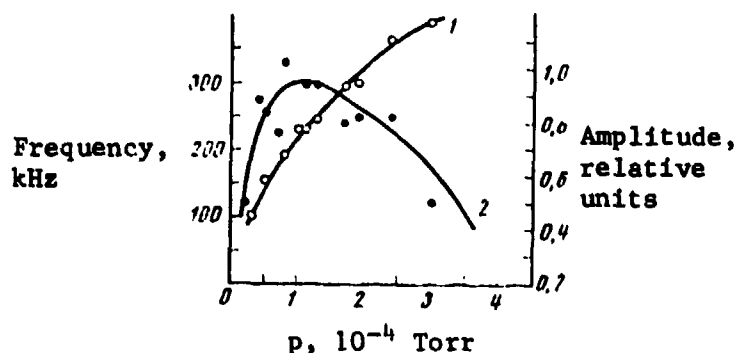


Fig. 31--Frequency (curve 1) and amplitude (curve 2) of ion oscillations as functions of air pressure where  $H^-$  beam current = 2 mA at 20 keV [84] (By permission of American Institute of Physics)

The interaction of a negative ion beam with the plasma electrons created by the ionization of a neutral gas by the same beam can affect the degree of neutralization and consequently the transport of the beam [87]. An added energy transfer from the beam ions to the plasma electrons accompanies the electron oscillation excitation and causes an increase in the positive beam potential along the axis [88,89]. This effect produces radial focusing of the ions in a negative ion beam and defocusing in a positive ion beam [88]. Plasma electron excitation by a negative ion beam, as for ion oscillations, shows dependence on pressure--although in a different frequency range. The frequency increased from 7 to 30 MHz in a pressure change from 1 to  $6 \times 10^{-4}$  Torr. In this region, the amplitude of the oscillations jumped by a factor of 4 to a sharp maximum at a pressure of  $5 \times 10^{-4}$  Torr, beyond which value the amplitudes demonstrated a sharp drop, caused by the collision of the charged particles with neutrals.

The effect of radial limitation of the system on the excitation of electron oscillations was demonstrated in [87] by using an iris diaphragm. Various size diaphragms determining the beam and plasma radii were used to measure spectra of the excitation oscillations. The dependence of the frequency and amplitude of the oscillations on the beam radius were measured at different pressures. These measurements demonstrated a rapid increase in the frequency and amplitude of the electron oscillations with increase in beam radius at pressures of 4 to  $5 \times 10^{-4}$  Torr and above. Below these pressures, the frequency and amplitude of the oscillations showed little change. Members of the team at IFANU concluded that the excitation of longitudinal electron oscillations depends greatly on the radial limitation of the system. They are currently investigating the effect of (1) radial plasma inhomogeneity on electron oscillation excitation and (2) oscillations on the degree of neutralization and transport of the beam.

In 1979, the Gabovich team investigated the transport of a high-current-density negative ion beam at  $J \sim 100 \text{ mA/cm}^2$  ( $1 \text{ mA/cm}^2$  in previous studies) [50]. Team members observed large deneutralization caused by beam instabilities at current densities of about  $50 \text{ mA/cm}^2$ , depending on the length of transport in gas. Figure 32 shows the

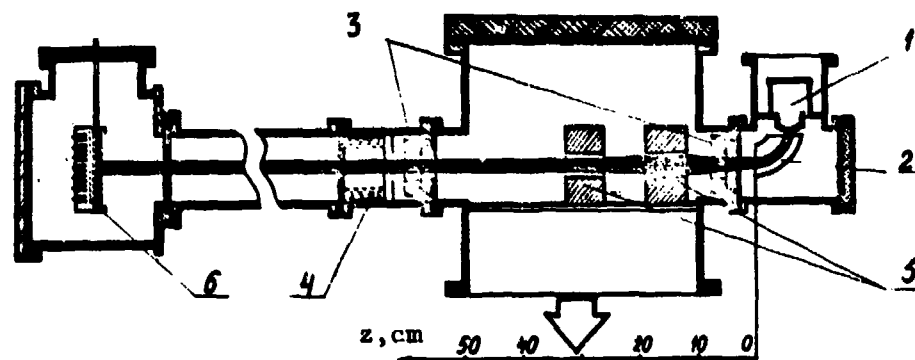


Fig. 32--Apparatus for high current density negative ion beam transport [50] (By permission of American Institute of Physics)

- 1--negative ion source
- 2--deflection magnet
- 3--Rogovsky loops
- 4--positive ion and electron analyzer
- 5--magnetic quadrupole lens
- 6--collectors

experimental apparatus used. An 80 mA, 15-keV  $H^-$  beam was formed with a current density of  $50 \text{ mA/cm}^2$  and a pulse duration of  $600 \mu\text{s}$ . The beam was injected into gas at pressures from  $2 \times 10^{-6}$  to  $10^{-4}$  Torr. The beam potential, measured by a specially designed capacitive probe, determined the degree of space charge neutralization. A Rogovsky loop was used to measure the beam current and a Faraday cup to measure the beam current density.

Beam potential oscillograms recorded at various positions along the beam (distance  $z$  in this case is measured from the magnet chamber) are shown in Fig. 33. The large negative potential at the beginning of each pulse (at small  $z$ 's) corresponded to a poor space charge neutralization of the beam. During this period, the beam is strongly defocused and partly lost to the chamber walls. With increased  $z$ , the potential, which is proportional to the beam current, decreased considerably.

Good beam neutralization was observed at small  $z$ 's after the elapse of the neutralization time  $\tau_n = (n_a \sigma_1 v_b)^{-1}$  (where  $n_a$  = concentration of atoms in the chamber,  $v_b$  = ion beam velocity, and  $\sigma_1$  = slow ion formation cross section caused by the collision of a

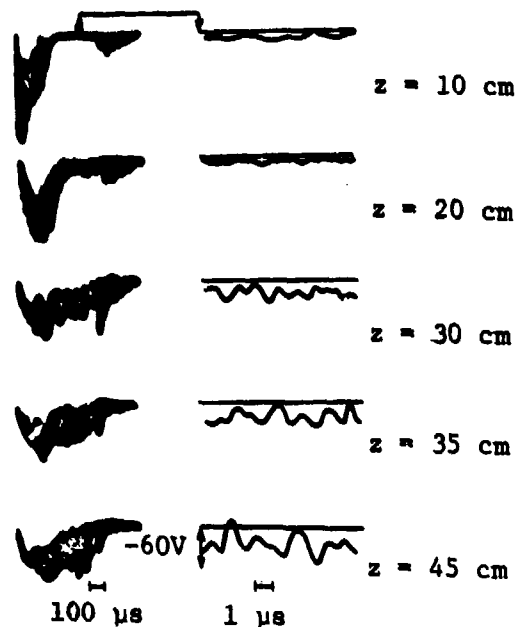


Fig. 33--Oscillograms showing beam potential as function of  $z$  with  $p = 2.5 \times 10^{-6}$  Torr (slow scan on left, fast scan on right) [50] (By permission of American Institute of Physics)

negative ion with an atom), during which time positive ions can be accumulated. At this point, the beam had neither large statistical and oscillatory fields nor current density pulsations (see Fig. 33). However, even at distances of 20 to 30 cm, the beam neutralization was lost. This loss was indicated by the appearance of oscillations of the negative potential, the amplitude of which increased to a value as high as 10 to 20 percent of the nonneutralized beam potential  $\Delta\phi = I_-/v_p$ , where  $I_-$  is the beam current with the given cross section.

IFANU's analysis of the data in [50] related the observed phenomena of ion-ion beam instabilities for the following reasons:

1. The oscillation amplitudes increased as the beam progressed along the beam line.
2. The Langmuir frequency of the neutralizing positive ions,  $f_+ = (e^2 n_+ / \pi M_+)^{1/2}$ , as calculated for corresponding beam current



density, was close to the characteristic frequency of the observed potential oscillations and had a value of about 1 MHz.

3. Current density signals, as measured by collectors located symmetrically about the beam axis 20 mm from each other, were found to be in opposite phase, demonstrating that the oscillations occurred perpendicular to the propagation of the beam.
4. At large distances ( $z$ ) the large potential oscillations were accompanied by oscillations of almost 100 percent in beam current density.

The amplitudes of the observed beam oscillations depended markedly on the gas pressure in the chamber, as shown in Fig. 34. Analysis showed that at low pressures ( $5 \times 10^{-6}$  to  $4 \times 10^{-5}$  Torr), the electrons that were formed quickly left the beam and the concentration of positive ions was very small:  $n_e/n_+ \approx 5 \times 10^{-4}$  to  $5 \times 10^{-3}$ . This analysis

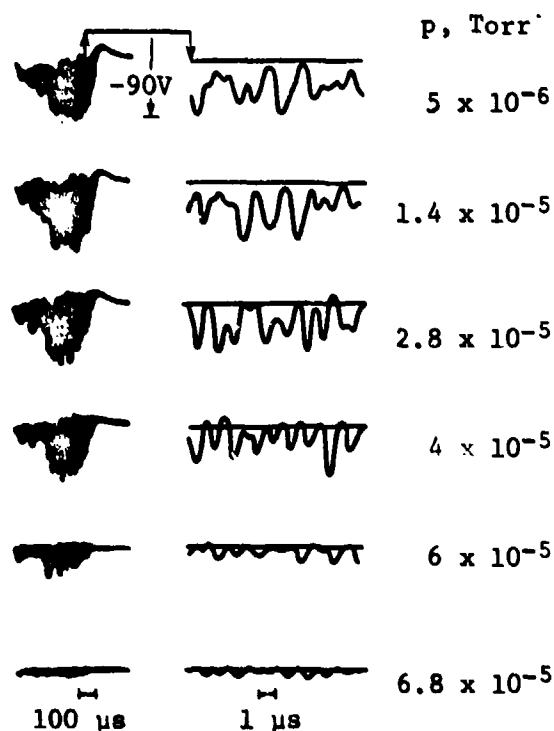


Fig. 34--Oscillograms showing beam potential as function of pressure with  $z = 50$  cm (slow scan on left, fast scan on right) [50] (By permission of American Institute of Physics)

explains the existence of the observed large amplitude oscillations and their nondependence on the gas in the low pressure range. With further increase in gas pressure, the beam potential changed from a negative to low positive value, at which point the electron concentration was comparable to that of the positive ions. Furthermore, the amplitude of the potential oscillations considerably decreased. IFANU concluded that, despite an absence of initial current oscillations, strong oscillations of the negative potential are generated in the neutralized negative ion beam because of ion-ion instabilities in the beam. The field associated with the instabilities can cause the beam to defocus and increase the beam emittance, thereby hindering the transport of intense negative ion beams at low gas pressures.

Continuing in 1980 to study the mechanism instrumental in the deneutralization of dense negative ion beams (beam density approximately  $50 \text{ mA/cm}^2$ ) passing through low pressure gas [90,91], researchers at IFANU demonstrated that high amplitude radial oscillations produced in the beam caused the radial dispersion of the positive ions, which have a rate of flow almost proportional to the amplitude of the oscillations. The above experimental results were obtained with the same apparatus that was used in previous experiments, modified by the addition of dosimetric equipment: specially designed beam probes, several Rogovsky loops, and variously apertured Faraday cups [50]. A cylindrical four-grid analyzer for slow particles measured the radial current component and the energy spectrum of the positive ions. The experiments used  $\text{H}^-$  beam currents up to 100 mA at 14 keV, with 600- $\mu\text{s}$  pulse length and a starting current density of approximately  $50 \text{ mA/cm}^2$ . The background gas pressures was regulated from a minimum of  $3 \times 10^{-6}$  Torr.

IFANU modulated the negative ion beam externally and observed the modulation's effect along the length of the beam. To modulate the radial velocity externally, an AC voltage was applied to a metal probe placed at the center of the beam at position  $z = 0$ . The length of the longitudinal wave generated along the beam was measured by noting the change in phase (along  $z$ ) of the potential oscillations set up by the external modulation. The wave length was observed to be  $\lambda_z = 25 \text{ cm}$ ,

with the longitudinal phase velocity  $v_{\phi_z} = \lambda_z f_{\text{mod}} = 1.8 \times 10^7$  cm/s, beam velocity  $v_b = 1.7 \times 10^8$  cm/s,  $f_{\text{mod}} = 0.7$  MHz, and modulating voltage = 125 V. The above measurements provided the first experimental evidence that the longitudinal phase velocity of the produced oscillations was considerably lower than velocity of the beam.

IFANU determined that the balance between the rate of positive ion production and the rate of their loss from the beam governed the depth of the negative potential well. This depth, in turn, determined the radial velocity and energy of the leaving positive ions. When ions leave only in the radial direction, the ion current is equated to the beam current as follows:  $I_+ = I_- \sigma_i n_a L$ , where  $I_-$  is the beam current,  $I_+$  is the radial positive ion current,  $L$  is the length of the beam trajectory,  $n_a$  is the concentration of atoms proportional to the background pressure, and  $\sigma_i$  is the ionization cross section of the gas. The measured experimental dependence of  $I_+$  on background pressure is shown in Fig. 35 for two locations along the beam.

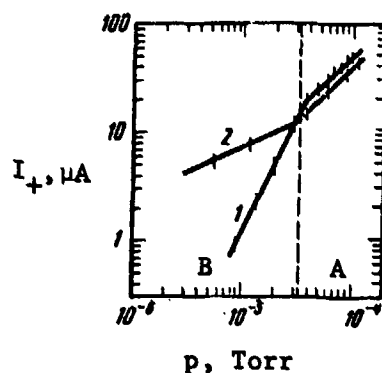


Fig. 35--Radial positive ion current ( $I_+$ ) as function of background pressure along beam line at  $z = 18$  cm (curve 1) and  $z = 38$  cm (curve 2) [90] (By permission of American Institute of Physics)

The data represent two separate, well-defined areas of pressure in which the character of the current dependence of the positive ions is substantially different. In the area of low pressures (region B in Fig. 35) at small  $z$ 's, the current is much lower than the value of the radial positive ion current of  $I_{+}\sigma_{i}n_{a}L$ ; at large  $z$ 's, the current is greater than this value. In the area of low pressures, the value of  $I_{+}$  increases considerably with the increase of  $z$  from 18 to 38 cm. At the minimum pressure this increase can be as high as one order of magnitude. In the area of higher pressures (region A in Fig. 35), the value of  $I_{+}$  does not depend on  $z$  but correlates with the ion production rate.

The above observations lead to the following explanation of the positive ion loss from the beam: At low gas pressures, ions that are formed at short distances from the source (small  $z$ ) move along the beam and have a very small radial current component. However, at large distances from the source (large  $z$ ), the ions formed move outward radially together with the ions formed at small  $z$ 's to create a radial current that is considerably greater than the current resulting from ion production [91].

Measurements of the electron current made at  $z = 18$  cm [91] demonstrated that the current can be represented by an expression analogous to the  $I_{+}$  equation stated above:  $I_{e} = I_{-}\sigma_{e}n_{a}L$  in which  $\sigma_{e} = \sigma_{i} + \sigma_{-10}$ . Here  $\sigma_{-10}$  is the electron detachment cross section for a negative ion collision with the background gas atoms. The relationship of the electron and ion currents in region A was experimentally determined to be  $I_{e}/I_{+} = 4$ . This ratio is close to the calculated value of  $I_{e}/I_{+} = \sigma_{e}/\sigma_{i} = 5$ , in which  $\sigma_{e} = 2 \times 10^{-15}$  cm<sup>2</sup> and  $\sigma_{i} = 4 \times 10^{-16}$  cm<sup>2</sup> for argon.

The energy spectrum of the ions leaving the beam radially was measured in [91] at various beam currents, background pressures, and locations along the beam path. The data for relatively low beam currents (15 to 20 mA) and a pressure of  $3 \times 10^{-5}$  Torr determined the positive ion formation energy to be only several eV. With a beam current of about 80 mA, the energy spread was in the tens-of-eV range. At low pressures, when the beam possesses a negative beam potential,

the spread in the ion energy, which is caused by oscillations of the beam potential, is proportional to the oscillation amplitudes. These measurements showed the direct dependence of the radial ion current on the oscillation amplitudes.

Recent Soviet papers demonstrate the existence of a large flow of positive ions along the negative ion beam at low gas pressures. This effect was shown to be linked to the radial oscillations of the neutralizing positive ions induced by the beam and to be the basic mechanism involved in the radial loss of positive ions.

## VI. CONCLUSIONS

Thanks to the development of intense surface-plasma-type ion sources in the USSR, the Soviets now have the capability to produce pulsed  $H^-$  ion beams of 100 to 150 mA with high brightness (up to  $10^8$  A/cm<sup>2</sup>-rad<sup>2</sup>). Although the Soviet literature does not reveal the values of the  $H^-$  DC beam currents produced by these sources, U.S. researchers [1] report that the Nuclear Physics Institute has produced an  $H^-$  DC beam of over 100 mA and is working toward a 1-A  $H^-$  DC beam. Researchers in the United States [92], however, note the low emittance measurements reported by the Soviets. The above values show Soviet capabilities to be at least on a par with current U.S. achievements in maximum ion beam output, as well as beam brightness and emittance, for both pulsed and DC continuous beam operation. Soviet researchers assert that present maximum operating values do not represent the limit of the surface plasma source output and that further development of the source will considerably improve the source emission characteristics, ion yields, and beam quality.

Soviet research has demonstrated that the behavior of the discharge in the source determines the ion-optical characteristics of the beam. Optimum operation of the source discharge can be obtained by adjusting the source parameters (magnetic field, hydrogen and cesium gas flow, electrode temperatures, etc.) to virtually eliminate oscillations in the discharge (i.e., to achieve noiseless operation). Random oscillations in the source discharge limit the minimum value of the normalized beam emittance to 3 to 5 x 10<sup>-2</sup> cm-mrad across and 0.1 to 0.2 cm-mrad along the emission slit. The corresponding minimal values of emittance achieved in a noise-free discharge were 3 x 10<sup>-3</sup> cm-mrad and 2 x 10<sup>-2</sup> cm-mrad, while the beam brightness increased by a factor of 100 over the noisy source operation.

The development of the semiplanotron surface-plasma ion source, together with modifications made in the planotron electrodes, led to better control of the discharge and a substantial increase in source power and gas efficiency. While making source gas flow efficiency

measurements, Soviet researchers observed a gas blocking mechanism when the plasma was sustained in front of the emission slit. The resulting decrease in pressure beyond the slit decreased the negative ion loss due to electron stripping and provided a high electric strength in the extraction-gap region.

Research on the hollow-beam surface-plasma source showed that in principle a symmetric hollow discharge could be maintained and used for the production of future high-current, hollow, negative ion beams (projected 3 A of  $H^-$ ).

By means of a PIG-type ion source, a 20-mA DC  $H^-$  ion beam was formed with low-level beam current oscillations (less than 0.05 percent). The oscillation amplitudes were found to be several orders of magnitude lower than the corresponding oscillations in a positive ion beam. The  $H^-$  ion beam was found to increase linearly with source pressure up to 0.1 Torr, whereas the  $H^+$  beam demonstrated weak pressure dependence.

The production of intense negative ion beams by the double charge exchange of a low-energy positive ion beam was also investigated. This method, using an 8-A positive hydrogen beam at 10 keV, provided 1.4 A of  $H^-$  at 40 keV with 10-ms pulse lengths. A multiple-slit positive ion source that does not use an external magnetic field was developed for double charge exchange. The source yields 30 A of  $H^+$  at 25 keV, with a 20-ms pulse length and a beam cross section of 8 by 18 cm<sup>2</sup>.

Investigating negative ion beam transport over large distances through gases at various pressures, Soviet researchers concentrated on basic mechanisms involved in space charge neutralization of the beam. The formation of neutralizing positive ions within the beam by the ionization of the background gas was analyzed as a function of gas pressure and distance along the beam. At low pressures and short distances from the ion source, a flow of positive ions traveling along the beam was observed to show very small radial current flows; however, positive ions formed at large distances were found to move only radially outward. These positive ion flows, formed at small and large distances, combine to create a total radial current considerably greater than the current resulting from ion production alone. Thus, at low pressures,

a large flow of positive ions along the negative ion beam was demonstrated experimentally. This flow explains the radial loss of positive ions from the beam. At high pressures, the radial positive ion current was found to be (1) independent of location along the beam and (2) represented by the ion production rate caused by the beam's ionization of background gas. Measurements of electron currents demonstrated an analogous condition to positive ion current dependence on beam current. At relatively high pressures (above  $3 \times 10^{-5}$  Torr), the ratio of electrons to positive ions formed within the beam was found to be 4 (for argon), as against the figure of 5 obtained from the ratio of the two ionization cross sections. The above data suggest that the Soviets are expending considerable effort on studying space charge neutralization of negative ion beams.

One Soviet report showed that gas focusing could be used only for relatively short beam-transport distances (up to 200 cm) at high pressures (approximately  $10^{-4}$  Torr), because of the reduction in beam current density caused by electron stripping. Good beam neutralization was observed at short distances from the source after an elapse of neutralization time during which positive ions could be accumulated. Beyond a distance of 30 cm, oscillations of the beam potential were observed to show loss of beam neutralization.

Studying other methods of negative ion beam focusing, the Soviets observed focusing experimentally when the beam interacted with ion and electron oscillations in the plasma created when the beam ionized the background gas.

The possibility of compressing negative ion beams either by gas focusing or interaction with collective plasma oscillations led Soviet researchers to conclude that negative ion beams are more easily transported over large distances than are positive ion beams. In addition, negative ions are more efficiently converted into neutral beams at high energies, and negative ion beams emitted from a PIG-type ion source have considerably lower beam current oscillations than do positive ion beams.



The research and development of the surface-plasma negative ion source has been centered at NPI since the source's creation in 1971. G. I. Dimov heads the team responsible for the research; V. G. Dudnikov and Yu. I. Bel'chenko are the principal investigators. The team has published papers on the surface-plasma source in the open literature since 1972, reaching a maximum of eight in 1977, but only three in 1979 and two in 1980-1981. Since 1977, however, the papers published by this team have revealed increasing attention to the investigation of plasma targets for the creation of neutral beams by stripping electrons from negative ion beams.

This change in research direction indicates that the team has taken the next step in the development of neutral particle beams. The decrease in papers on source development in the past two years can be explained as either the acceptable fulfillment of the project's goals and termination of the investigations and start-up of the next phase of development, namely, electron stripping targets, or the imposition of security classification on any further ion source developments. Whatever the reason for it, the silence contrasts dramatically with the reporting of Western research, as exemplified by the publication in 1980 of the Proceedings of the Second International Symposium on the Production and Neutralization of Negative Hydrogen Ions and Beams at the Brookhaven National Laboratory.

A team headed by V. L. Komarov at the Yefremov Institute is the only other Soviet group publishing research on the surface-plasma source itself. This team's limited effort on the axially symmetric hollow beam source ended in 1978.

The research at IFANU concentrated specifically on the transport of negative ion beams involving space charge neutralization and focusing conditions; the IFANU team was not involved, however, in the ion source development project and did not interact with the other research teams mentioned in this report.

The IFTT team headed by B. A. D'yachkov, also unconnected with the other teams mentioned, has lately concentrated on the development of alkali-metal-vapor targets for use in transforming intense positive ion beams into negative ion beams by double charge exchange. These

targets are to be used in the neutral beam injectors for tokamaks and magnetic traps, which are being developed at the Kurchatov Atomic Energy Institute in Moscow. Earlier work by the IFTT team involved neutral beam formation by electron stripping of negative ions, the development of beam neutralizers, and the measurement of electron capture and electron detachment cross sections. The investigations being conducted at IFTT, NPI, and other research institutes on the formation of neutral beams by electron stripping of negative ion beams, development of beam neutralizers, and charge-exchange targets for conversion of positive to negative ion beams will be described in detail in a forthcoming Rand report.

REFERENCES

AE	<i>Atomnaya energiya</i>
DAN SSSR	<i>Doklady Akademii nauk SSSR</i>
FP	<i>Fizika plazmy</i>
Izv AN SSSR	<i>Izvestiya Akademii nauk SSSR, Seriya fizicheskaya</i>
PTE	<i>Pribory i tekhnika eksperimenta</i>
UFZh	<i>Ukrainskiy fizicheskii zhurnal</i>
ZhETF	<i>Zhurnal eksperimental'noy i teoreticheskoy fiziki</i>
ZhETF, Pis'ma	<i>Pis'ma v Zhurnal eksperimental'noy i teoreticheskoy fiziki</i>
ZhTF	<i>Zhurnal tekhnicheskoy fiziki</i>
ZhTF, Pis'ma	<i>Pis'ma v Zhurnal tekhnicheskoy fiziki</i>

1. Hiskes, J., private communication.
2. Prelec, K., "Development of  $H^-$  Sources at Brookhaven National Laboratory," Proceedings of the Symposium on the Production and Neutralization of Negative Hydrogen Ions and Beams, Brookhaven National Laboratory, BNL-50727, September 26-30, 1977, p. 111.
3. Sluyters, Th., and K. Prelec, "High Energy Neutral Injectors Based Upon Negative Ion Plasma Sources," in Proceedings ..., BNL-50727, 1977, p. 280.
4. Sluyters, Th., and C. Lam, "Present Status of Negative Ion Acceleration and Transportation from SP Sources," in Proceedings ..., BNL-50727, 1977, p. 211.
5. Prelec, K., and Th. Sluyters, "A Pulsed Negative Hydrogen Source for Currents up to One Ampere," IEEE Trans. on Nuc. Science, NS-22, No. 3, June 1975, p. 1662.
6. Prelec, K., "Progress in the Development of High Current, Steady State  $H^-/D^-$  Sources at BNL," Proceedings of the Second International Symposium on the Production and Neutralization of Negative Hydrogen Ions and Beams, Brookhaven National Laboratory, BNL-51304, October 6-10, 1980, p. 145.
7. Alessi, J., and Th. Sluyters, "Regular and Asymmetric Negative Ion Magnetron Sources with Grooved Cathodes," in Proceedings ..., BNL-51304, 1980, p. 153.
8. Sluyters, Th., and J. Alessi, "Extraction and Transport of  $H^-$ ,  $D^-$  Beams from Magnetron Sources," in Proceedings ..., BNL-51304, 1980, p. 166.

9. Herscovitch, A., and K. Prelec, "Mark V Magnetron with H.C.D. Plasma Injection," in Proceedings ..., BNL-51304, 1980, p. 160.
10. Allison, P. W., "Experiments with a Dudnikov-Type  $H^-$  Ion Source," in Proceedings ..., BNL-50727, 1977, p. 119.
11. -----, "A Direct Extraction  $H^-$  Ion Source," IEEE Trans. on Nuc. Science, NS-24, No. 3, June 1977, p. 1594.
12. Allison, P., H. V. Smith, Jr., J. D. Sherman, " $H^-$  Ion Source Research at Los Alamos," in Proceedings ..., BNL-51304, 1980, p. 171.
13. Sherman, J. D., P. Allison, H. V. Smith, Jr., " $H^-$  Beam Formation from a Penning Surface Plasma Source Using Circular Emission-Extractor Electrodes," in Proceedings ..., BNL-51304, 1980, p. 184.
14. Smith, H. V., P. Allison, J. D. Sherman, "A Rotating Penning Surface-Plasma Source for DC  $H^-$  Beams," in Proceedings ..., BNL-51304, 1980, p. 178.
15. Fasolo, J. A., " $H^-$  Source Development at ANL," IEEE Trans. on Nuc. Science, NS-24, No. 3, June 1977, p. 1597.
16. -----, "Progress Report on Zero Gradient Synchrotron  $H^-$  Source Development," IEEE Trans. on Nuc. Science, NS-22, No. 3, June 1975, p. 1665.
17. Schmidt, C. W., and C. D. Curtis, "A 50 mA Negative Hydrogen Ion Source," IEEE Trans. on Nuc. Science, NS-26, No. 3, June 1979, p. 4120.
18. -----, "Proceedings of the 1976 Proton Linear Accelerator Conference," Chalk River Nuclear Laboratory, Ontario, AECL 6577, 1976, p. 402.
19. -----, "An  $H^-$  Ion Source for Accelerator Use," in Proceedings ..., BNL-50727, 1977, p. 123.
20. Schmidt, C. W., "Operation of the Fermilab  $H^-$  Magnetron Source," in Proceedings ..., BNL-51304, 1980, p. 189.
21. Curtis, C. D., G. M. Lee, C. W. Owen, C. W. Schmidt, W. M. Smart, "Linac  $H^-$  Beam Operation and Uses at Fermilab," IEEE Trans. on Nuc. Science, NS-26, No. 3, June 1979, p. 3760.
22. Ehlers, K. W., private communication.
23. Ehlers, K. W., K. N. Leung, "A Multicusp Negative Ion Source," LBL-10013 Preprint, October 1979.

24. -----, "Characteristics of a Self-Extraction Negative Ion Source," in Proceedings ..., BNL-51304, 1980, p. 198.
25. Leung, K. N., K. W. Ehlers, " $H^-$  Ion Formation from a Surface Conversion Type Ion Source," in Proceedings ..., BNL-51304, 1980, p. 65.
26. Bel'chenko, Yu. I., G. I. Dimov, V. G. Dudnikov, A. A. Ivanov, "Formation of Negative Ions in a Gas Discharge," DAN SSSR, Vol. 213, No. 6, 1973, p. 1283.
27. Bel'chenko, Yu. I., G. I. Dimov, V. G. Dudnikov, "Intense  $H^-$  Ion Beam from a Discharge in Crossed Fields," ZhTF, Vol. 43, No. 8, 1973, p. 1720.
28. -----, "A Powerful Injector of Neutrals with a Surface-Plasma Source of Negative Ions," Nuclear Fusion, Vol. 14, 1974, p. 113.
29. -----, "Negative Ion Surface-Plasma Source," ZhTF, Vol. 45, No. 1, 1975, p. 68.
30. -----, "Physical Principles of the Surface-Plasma Method for Producing Beams of Negative Ions," in Proceedings ..., BNL-50727, 1977, p. 79.
31. Dudnikov, V. G., Ye. G. Obrazovskiy, G. I. Fiksel', "Electron Emission Characteristics of Surface Plasma Sources and the Effective Generation of  $H^-$  Ions," FP, Vol. 4, No. 3, 1978, p. 662.
32. Dudnikov, V. G., "Some Effects of Surface-Plasma Mechanism for Production of Negative Ions," in Proceedings ..., BNL-51304, 1980, p. 137.
33. Bel'chenko, Yu. I., G. I. Dimov, V. G. Dudnikov, "Emission of an Intense Flow of Negative Ions from Surfaces Bombarded by Fast Particles of a Discharge," Izv AN SSSR, Vol. 37, No. 12, 1973, p. 2573.
34. Derevyankin, G. Ye., V. G. Dudnikov, "Formation of  $H^-$  Ion Beams with Surface-Plasma Sources for Accelerators," Preprint IYaF (Institute of Nuclear Physics) 79-17, March 1979.
35. Derevyankin, G. Ye., V. G. Dudnikov, P. A. Zhuravlev, "Electromagnetic Valve for Pulsed Gas Flow," PTE, No. 5, 1975, p. 168.
36. Strokach, A. P., K. N. Klochkov, "Electromagnetic Valve for Pulsed Introduction of Gas into Vacuum Systems," PTE, No. 1, 1980, p. 251.
37. Bel'chenko, Yu. I., V. G. Dudnikov, "Surface-Plasma Source Without a Closed Electron Drift Path Called a Semiplanotron," Preprint IYaF 78-95, November 1978.

38. Komarov, V. L., A. P. Strokach, "Experimental Investigation of a Hollow Beam Negative Ion Source," ZhTF, Vol. 49, No. 4, 1979, p. 750.
39. Bel'chenko, Yu. I., V. I. Davydenko, G. Ye. Derevyankin, A. F. Dorogov, V. G. Dudnikov, "Emission of Cesium from a Surface-Plasma  $H^-$  Ion Source," ZhTF, Pis'ma, Vol. 3, No. 14, 1977, p. 693.
40. Apolonskiy, A. N., Yu. I. Bel'chenko, G. I. Dimov, V. G. Dudnikov, "Gas Efficiency of Surface-Plasma Sources of Negative Hydrogen Ions," ZhTF, Pis'ma, Vol. 6, No. 2, 1980, p. 86.
41. Grossman, M. W., " $H^-$  Ion Source Diagnostics," in Proceedings ..., BNL-50727, 1977, p. 105.
42. Bel'chenko, Yu. I., G. I. Dimov, V. G. Dudnikov, "Hydrogen Cut-off in Surface-Plasma Sources," Soviet-American Conference on Neutral Injectors Using Negative Ions, Moscow, 1977.
43. Dimov, G. I., G. Ye. Derevyankin, V. G. Dudnikov, "A 100 mA Negative Hydrogen Ion Source for Accelerators," IEEE Trans. on Nuc. Science, NS-24, No. 3, June 1977, p. 1545.
44. Derevyankin, G. Ye., V. G. Dudnikov, V. S. Klenov, "Ion-Optical Characteristics of  $H^-$  Ion Beams Generated by Surface Plasma Sources," ZhTF, Vol. 48, No. 2, 1978, p. 404.
45. Prelec, K., Th. Sluyters, Review of Scient. Instr., Vol. 44, 1973, p. 145.
46. Gabovich, M. D., Yu. N. Kozyrev, A. P. Nayda, L. S. Simonenko, I. A. Soloshenko, " $H^-$  Ion Beam Limit from a DC Plasma Source," ZhTF, Pis'ma, Vol. 4, No. 7, 1978, p. 378.
47. Gabovich, M. D., A. P. Nayda, F. M. Isayev, UFZh, Vol. 15, 1970, p. 667.
48. Gabovich, M. D., Yu. N. Kozyrev, A. P. Nayda, "20 mA DC  $H^-$  Ion Source with a Low Level of Beam Pulsation," PTE, No. 2, 1980, p. 45.
49. Gabovich, M. D., I. M. Mitropan, "An Intense Antimony Negative Ion Source," PTE, No. 5, 1976, p. 181.
50. Gabovich, M. D., D. G. Dzhabbarov, A. P. Nayda, "The Effect of Deneutralization of a Dense Negative Ion Beam," ZhETF, Pis'ma, Vol. 29, No. 9, 1979, p. 536.
51. Krylov, A. I., V. V. Kuznetsov, N. N. Semashko, "Physics Considerations of Injector Systems for Large Tokamaks and Open Traps," AE, Vol. 48, No. 3, 1980, p. 186.

52. Semashko, N. N., V. V. Kuznetsov, A. I. Krylov, "Production of Negative Hydrogen Ion Beams by Double Charge Exchange," in Proceedings ..., ENL-50727, 1977, p. 170.
53. Kulygin, V. M., A. A. Panasenkov, N. N. Semashko, I. A. Chukhin, "Ion Source Without an External Magnetic Field--IBM-5," ZhTF, Vol. 49, No. 1, 1979, p. 168.
54. D'yachkov, B. A., V. I. Zinenko, "Charge Exchange of 5 to 40 keV Protons in Dense Vapor Streams of Lithium, Sodium, Magnesium, and Zinc," AE, Vol. 24, No. 1, 1968, p. 18.
55. D'yachkov, B. A., "Production of High Energy Neutrals by Conversion of  $H_1^-$ ,  $H_2^+$ , and  $H_3^+$  Ions in Ultrasonic Lithium Vapor Stream," ZhTF, Vol. 38, No. 8, 1968, p. 1259.
56. D'yachkov, B. A., S. M. Krivoruchko, V. Yu. Petrusha, "Emission of Lithium from a Supersonic Vapor Stream," ZhTF, Vol. 39, No. 5, 1969, p. 918.
57. D'yachkov, B. A., V. I. Zinenko, "Development of an Intense  $He^-$  Ion Source," ZhTF, Vol. 41, No. 2, 1971, p. 404.
58. D'yachkov, B. A., V. I. Zinenko, M. A. Pavliy, "Formation of  $H^-$  Ions by Charge Exchange of Protons of 1.5 to 10 keV Energy in Dense Li, Na, K, and Mg Vapor Streams," ZhTF, Vol. 41, No. 11, 1971, p. 2353.
59. D'yachkov, B. A., V. I. Zinenko, A. V. Nasonov, "Apparatus for Measuring the Conversion Coefficient of Low Energy Positive Ions into Negative Ions," PTE, No. 5, 1975, p. 27.
60. Dimov, G. I., G. V. Roslyakov, "Pulsed Charge Exchange Source of Negative Hydrogen Ions," PTE, No. 1, 1974, p. 29.
61. D'yachkov, B. A., V. M. Nesterenko, V. Yu. Petrusha, "Lithium Ion Neutralizer," PTE, No. 2, 1974, p. 35.
62. D'yachkov, B. A., V. I. Zinenko, M. A. Pavliy, V. Yu. Petrusha, "A Sodium Charge Exchange Target with a Large Aperture," PTE, No. 5, 1978, p. 37.
63. Dimov, G. I., G. V. Roslyakov, "A 20 mA Negative Hydrogen Ion Beam Injector," PTE, No. 2, 1974, p. 33.
64. Dimov, G. I., A. A. Ivanov, G. V. Roslyakov, "Electron Loss of Fast  $H^-$  Ions and  $H^0$  Atoms in a Plasma Target," ZhTF, Vol. 47, No. 9, 1977, p. 1881.
65. Dimov, G. I., V. G. Dudnikov, "Control of Particle Flow by Charge Exchange," FP, Vol. 4, No. 3, 1978, p. 692.

66. Dimov, G. I., Preprint IYaF 304, Novosibirsk, 1969.
67. Dimov, G. I., G. V. Roslyakov, Nuclear Fusion, No. 15, 1975, p. 551.
68. Fink, I. E., W. L. Barr, G. W. Hamilton, LLL Report, UCRP-52173, 1976.
69. Van Zyl, B., N. G. Utterback, R. C. Amme, Rev. of Scient. Instr., No. 47, 1976, p. 814.
70. McGeoch, M. W., "Laser Neutralization of Negative Ion Beams for Fusion," in Proceedings ..., BNL-51304, 1980, p. 304.
71. D'yachkov, B. A., V. I. Zinenko, "Production of Neutral Atoms of C, O, F, Cl with Energy of 110-380 keV by Means of Electron Detachment from Negative Ions," ZhTF, Vol. 46, No. 2, 1976, p. 297.
72. D'yachkov, B. A., V. I. Zinenko, G. V. Kazantsev, "Measurement of the Scattering Angle of Neutrals Obtained by the Stripping of Negative Hydrogen Ions," ZhTF, Vol. 47, No. 2, 1977, p. 416.
73. Dimov, G. I., A. A. Ivanov, G. V. Roslyakov, "Investigation of a Hydrogen Plasma Target," FP, Vol. 6, No. 4, 1980, p. 933.
74. Dimov, G. I., G. V. Roslyakov, V. Ya. Savkin, "Diagnostic Hydrogen Atom Injector," PTE, No. 4, 1977, p. 29.
75. Gabovich, M. D., A. P. Nayda, I. M. Protsenko, L. S. Simonenko, I. A. Soloshenko, "Gas Focusing of a Negative Ion Beam," ZhTF, Vol. 44, No. 4, 1974, p. 861.
76. Gabovich, M. D., L. S. Simonenko, I. A. Soloshenko, "Space Charge Neutralization of an Intense Negative Ion Beam," ZhTF, Vol. 48, No. 7, 1978, p. 1389.
77. Gabovich, M. D., "Space Charge Neutralized Ion Beams," UFZh, Vol. 24, No. 2, 1979, p. 257.
78. Gabovich, M. D., "Neutralized Ion Beams," Znaniye, No. 1, 1980.
79. Gabovich, M. D., I. A. Soloshenko, A. A. Goncharov, "Ion Langmuir Oscillations in an Ion Beam Plasma," ZhTF, Vol. 43, No. 11, 1973, p. 2292.
80. Neslin, M. V., Plasma Physics, No. 10, 1968, p. 377.
81. Panasenkov, A. A., N. N. Semashko, "A Fast Hydrogen Atom Injector," ZhTF, Vol. 40, 1970, p. 2525.



82. Simonenko, L. S., I. A. Soloshenko, "Self-Focusing of a Negative Ion Beam During Excitation of Ion Oscillations of a Plasma," FP, Vol. 4, No. 4, 1975, p. 635.
83. Katsubo, L. P., V. P. Kovalenko, I. A. Soloshenko, "Space-Time Ion Beam Focusing During Excitation of Langmuir Transverse Ion Oscillations of a Plasma," ZhETF, Vol. 67, No. 1(7), 1974, p. 110.
84. Gabovich, M. D., L. S. Simonenko, I. A. Soloshenko, V. N. Shkorina, "Excitation of Ion Plasma Oscillations by a Negative Ion Beam," ZhETF, Vol. 67, No. 5(11), 1974, p. 1710.
85. Gabovich, M. D., I. A. Soloshenko, "Excitation of Electron Langmuir Oscillations by an Ion Beam," ZhTF, Vol. 41, 1971, p. 1627.
86. Gabovich, M. D., I. A. Soloshenko, L. S. Simonenko, "Nonlinear Interaction of a Fast Ion Beam with Plasma Electrons," ZhETF, Vol. 62, No. 4, 1972, p. 1369.
87. Simonenko, L. S., I. A. Soloshenko, N. V. Shkorina, "Excitation of Electron Plasma Oscillations by a Negative Ion Beam," UFZh, Vol. 19, No. 11, 1974, p. 1886.
88. Gabovich, M. D., I. A. Soloshenko, "Effect of Electron Langmuir Oscillations Upon the Degree of Neutralization of an Ion Beam," ZhTF, Vol. 43, No. 8, 1973, p. 1656.
89. Gabovich, M. D., "Self-Deneutralization of a Quasi-neutral Ion Beam," UFZh, Vol. 19, No. 4, 1974, p. 692.
90. Dzhabbarov, D. G., A. P. Nayda, "Development of Instabilities in a Dense Negative Ion Beam in a Low Pressure Gas," ZhETF, Vol. 78, No. 6, 1980, p. 2259.
91. -----, "Movement of Positive Ions in a Plasma Formed by a Dense Negative Ion Beam in a Gas," FP, Vol. 6, No. 3, 1980, p. 577.
92. Allison, P. W., private communication.